OCT 1 9 1964

SECRET

UNCLASSIFIED

NAA-SR-9642
COPY 126 OF 275
47 PAGES
SERIES A

MASTER

S-RD Classification Confirmed. 11-2-71.

SNAP 8 EXPERIMENTAL REACTOR CRITICAL EXPERIMENT

(Title Unclassified)

AEC Research and Development Report

~~RESTRICTED DATA~~

This document contains restricted data as defined in the Atomic Energy Act of 1954. Its transmittal or the disclosure of its contents in any manner to an unauthorized person is prohibited.

This document contains Secret-Restricted Data relating to civilian applications of atomic energy.

GROUP I

Excluded from automatic downgrading and declassification

1 7339

ATOMICS INTERNATIONAL

A DIVISION OF NORTH AMERICAN AVIATION, INC.

UNCLASSIFIED

SECRET

DISTRIBUTION OF THIS DOCUMENT IS UNLIMITED

Printed in USA Price $1.05 Available from the

U. S. Atomic Energy Commission
Technical Information Extension,
P. O. Box 1001
Oak Ridge, Tennessee.

Please direct to the same address inquiries covering the procurement of other classified AEC reports.

UNCLASSIFIED

Exempt from CCRP Re-review Requirements
(per 7/22/82 Duff/Caudle memorandum) 5/3/04

NAA-SR-9642
SNAP REACTOR,
SNAP PROGRAM
M-3679 (35th Ed.)

Classification cancelled (or changed to UNCLASSIFIED
letter 4/17/73 Feldman DIV of Class. Wash DC
by authority of Brann
by GG DTIE, date 5/24/73

SNAP 8 EXPERIMENTAL REACTOR CRITICAL EXPERIMENT

(Title Unclassified)

STAFF
COMPACT SYSTEMS DIVISION

D.E. CROUTER, EDITOR

~~RESTRICTED DATA~~

This documen... defined in the Atomic Energy Act of ... mittal or the disclosure of its conte... unauthorized person is prohi...

This docum... Secret-Restricted Data relating to civilian applic...s of atomic energy.

ATOMICS INTERNATIONAL

A DIVISION OF NORTH AMERICAN AVIATION, INC.
P.O. BOX 309 CANOGA PARK, CALIFORNIA

UNCLASSIFIED

CONTRACT: AT(11-1)-GEN-8
ISSUED: SEPTEMBER 15, 1964

~~SECRET~~

DISTRIBUTION OF THIS DOCUMENT IS UNLIMITED

DISTRIBUTION

SYSTEMS FOR NUCLEAR AUXILIARY POWER (SNAP)-REACTOR SNAP PROGRAM M-3679 (35th Ed.)

	Copy No
Aerojet-General Corporation (NASA)	1-6
Aerojet-General Corporation, Sacramento	7
Aerojet-General Nucleonics	8
Aeronautical Systems Division	9-10
Aerospace Corporation	11
Aerospace Test Wing (AFSC)	12
Air Force Surgeon General	13
Air Force Weapons Laboratory	14-15
AiResearch Manufacturing Company, Phoenix	16
Army Ballistic Research Laboratories	17
Army Missile Command	18
Army Nuclear Defense Laboratory	19
ARO, Inc.	20
Air University Library	21
Argonne National Laboratory	22
Army Combat Developments Command	23
Astropower, Inc.	24
Avco Corporation	25
Battelle Memorial Institute	26
Bendix Corporation (AF)	27
Brookhaven National Laboratory	28
Bureau of Naval Weapons	29-30
Bureau of Ships	31-32
Bureau of Yards and Docks	33
California Patent Group	34
Central Intelligence Agency	35
Chicago Patent Group	36
Defense Atomic Support Agency, Sandia	37
Department of the Army	38
Director of Defense Research and Engineering (OAP)	39
Edgerton, Germeshausen and Grier, Inc , Goleta	40
Foreign Technology Division (AFSC)	41
General Atomic Division	42
General Dynamics/Astronautics (AF)	43
General Dynamics/Fort Worth	44
General Electric Company, Cincinnati	45
General Electric Company (FPD)	46-47
General Electric Company (MSVD)	48
General Electric Company, Richland	49-50
General Electric Company, San Jose	51
General Electric Company, San Jose (AF)	52
General Technologies Corporation	53
Institute for Defense Analysis	54
Ion Physics Corporation	55
Jet Propulsion Laboratory	56-57
Johns Hopkins University (APL)	58
Lockheed-Georgia Company	59
Lockheed Missiles and Space Company	60
Los Alamos Scientific Laboratory	61
Martin-Marietta Corporation, Denver	62
Monsanto Dayton Laboratory	63
Mound Laboratory	64
ASA Ames Research Center	65
ASA Goddard Space Flight Center	66-67
ASA Langley Research Center	68
NASA Lewis Research Center	69-72
NASA Manned Spacecraft Center	73
NASA Marshall Space Flight Center	74
NASA Scientific and Technical Information Facility	75-77
National Aeronautics and Space Administration, Washington	78-79
NASA Western Operations Office	80
Naval Air Development Center	81
Naval Ordnance Laboratory	82-83
Naval Postgraduate School	84
Naval Radiological Defense Laboratory	85
Naval Research Laboratory	86 87
Naval Underwater Ordnance Station	88
Navy Marine Engineering Laboratory	89
New York Operations Office	90
New York Operations Office, Canel Project Office	91
North American Aviation, Inc., Downey	92
Nuclear Metals, Inc	93
Office of Naval Research	94-95
Office of the Assistant General Counsel for Patents (AEC)	96
Office of the Chief of Engineers	97
Office of the Chief of Naval Operations	98-100
Office of the Chief of Naval Operations (OP-03EG)	101-102
Office of the Chief of Transportation	103
Phillips Petroleum Company (NRTS)	104-107
Pratt and Whitney Aircraft Division	108
Pratt and Whitney Aircraft Division (NASA)	109
Rand Corporation	110
Republic Aviation Corporation	111
Sandia Corporation	112
School of Aerospace Medicine	113
Union Carbide Corporation (ORNL)	114-121
USAF Headquarters	122
University of California, Livermore	123
Westinghouse Electric Corporation (NASA)	124
Westinghouse Electric Corporation, Lima (AF)	125
Division of Technical Information Extension	126-165
AI Library (Includes 2 copies to CPAO, 2 copies to AEC, Washington, 2 copies to COO)	166-275

CONTENTS

TABLES

FIGURES

FIGURES

ABSTRACT

A prototype reactor core and reflector assembly manufactured for the SNAP 8 Experimental Reactor was subjected to a series of dry critical experiments prior to final assembly and power operation. Experimental results are interpreted in terms of: (a) the critical fuel loading, (b) the effects of reflector thickness, (c) the control element reactivity worths, (d) the effects of varying fuel and moderator densities, (e) the reactivity worths of special fuel and absorber rods, (f) the reactivity worths of the internal reflectors, (g) the β_{eff}/ℓ ratio, and (h) the power density distributions.

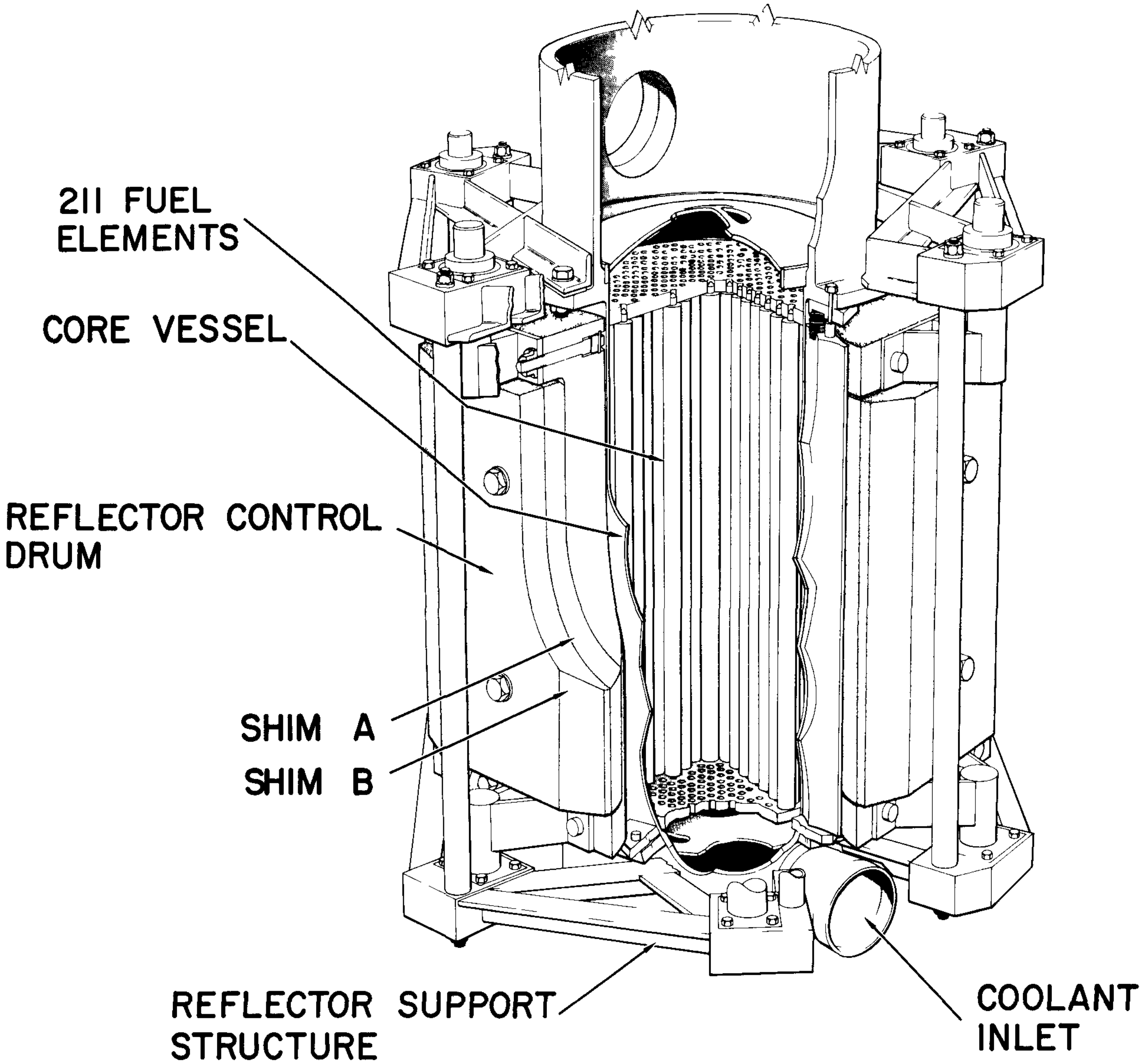

2-15-62 7570-80108A

Figure 1. SNAP 8 Experimental Reactor Cutaway

I. INTRODUCTION

A. SNAP 8 PROGRAM

SNAP 8 is a compact nuclear powerplant intended to produce approximately 35 kw of electric power output for use in spacecraft. The system, which is being developed jointly by NASA and AEC, employs a nuclear reactor (being developed by Atomics International under contract to the AEC) as a heat source for a mercury-Rankine cycle power conversion system (being developed by Aerojet-General Corporation under contract to NASA).

The SNAP 8 reactor is fueled and moderated by uranium-zirconium hydride and is cooled by eutectic NaK. Design objectives for the SNAP 8 reactor include a power output of 600 kwt at a NaK coolant outlet temperature of 1300°F for 10,000 hours operation.

B. S8ER PROGRAM

The SNAP 8 Experimental Reactor (S8ER) is the first of a series of three SNAP 8 reactors to undergo nuclear testing at Atomics International. The S8ER program is a test of the reactor only, without power conversion. The test objectives are to demonstrate reactor operation and to determine reactor performance characteristics over a wide range of power levels and core temperatures up to and including design conditions of 600 kwt, 1300°F. Reactor design principles will be verified and detailed experimental data will be provided upon which to base the final design of the flight reactor. The S8ER, shown in Figure 1 and described in Reference 1, is therefore similar to the flight reactor in size and configuration.

Prior to the final assembly and installation of the core in the Power Test Facility, a dry critical experimental program was completed to obtain a reactivity "calibration" of the reactor components. These experiments are described in this report. The relationships of experimental results to design calculations are indicated.

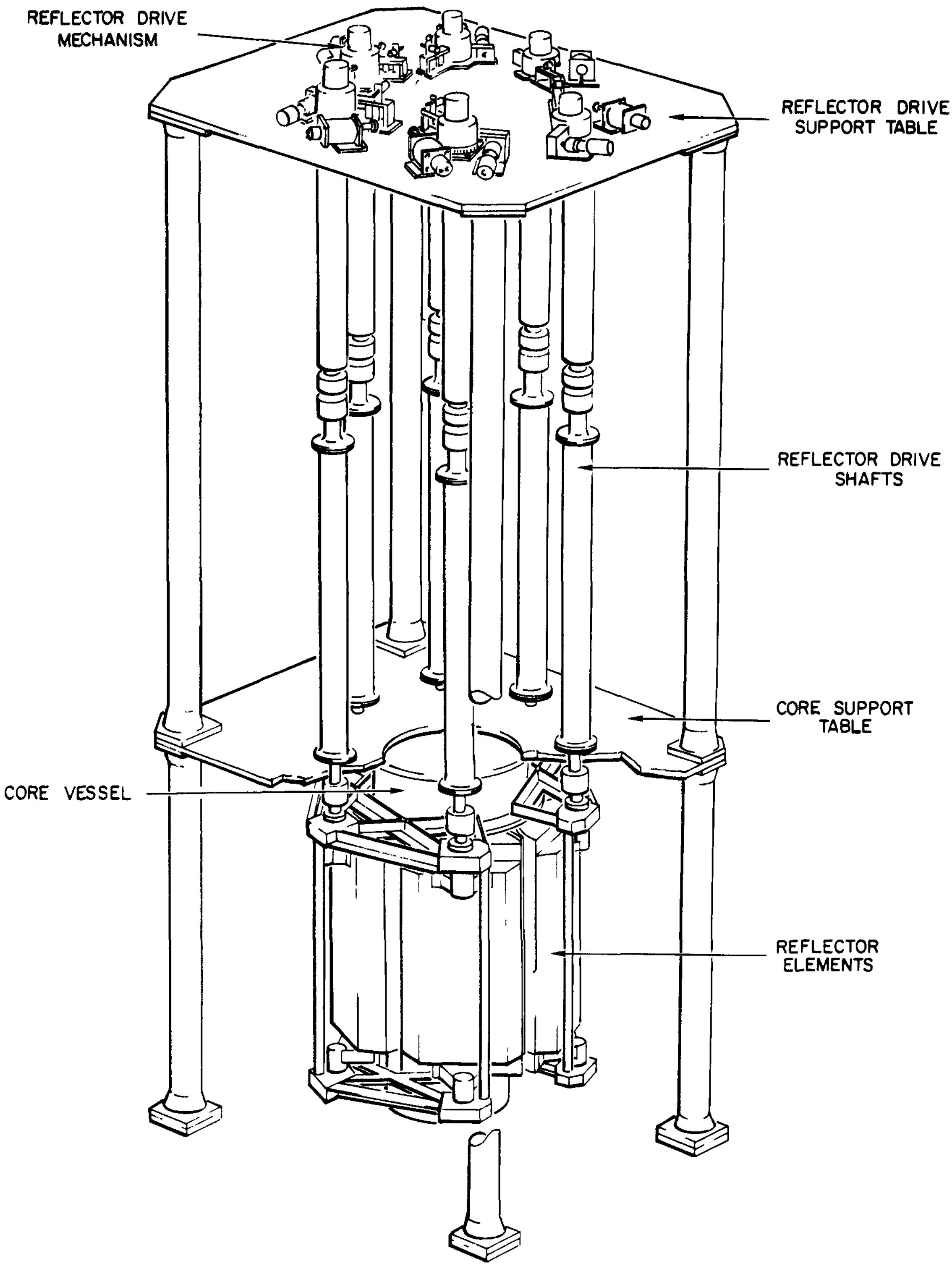

6-12-62 7570-5509

Figure 2. Critical Machine

II. DESCRIPTION

A. SITE AND FACILITY

The S8ER Dry Critical Experiments were conducted in the SNAP Critical Facility, Bldg 373, located at the North American Aviation Field Test Area, approximately 30 miles west-northwest of downtown Los Angeles. The critical machine, shown in Figure 2, was installed in the test cell as shown in Figure 3.

The critical machine consists of two tables, one arranged above the other. The core and reflector assembly are suspended below the lower table, while the upper table supports the drive mechanisms for the reflector control elements. Core loading changes were achieved manually by inserting or removing core and test components through the opening in the lower table (see Figure 4).

Prior to fuel loading, structures of previous critical machines were removed from the test cell and the S8ER critical machine was installed. The components were then checked, adjusted and/or thoroughly performance tested as

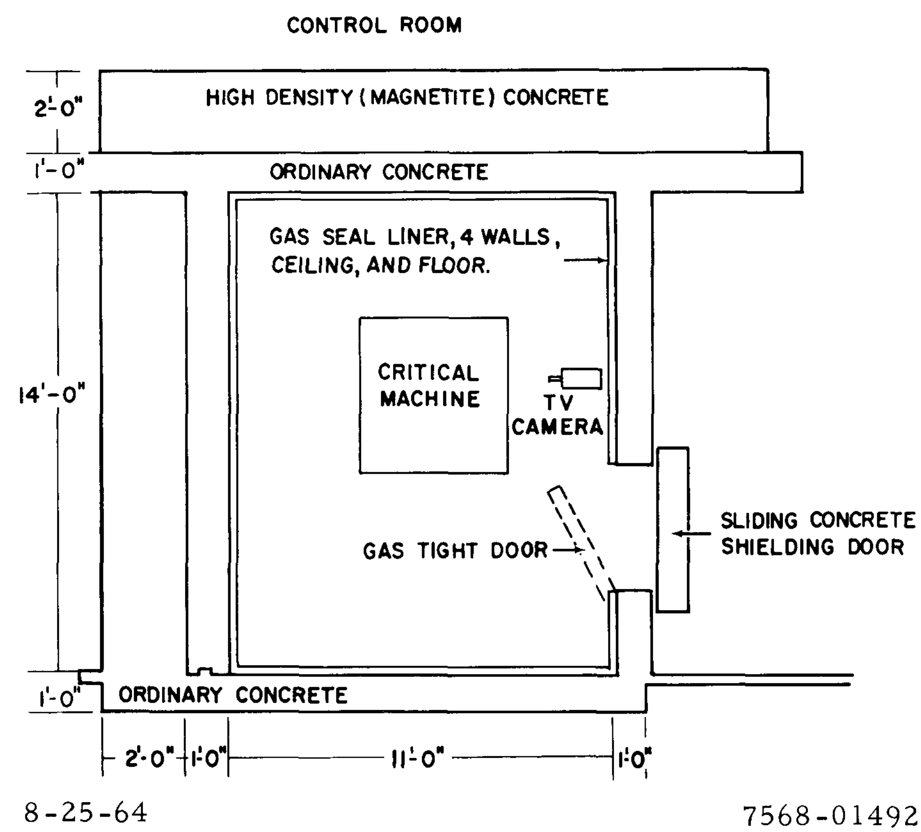

Figure 3. Critical Assembly Test Cell

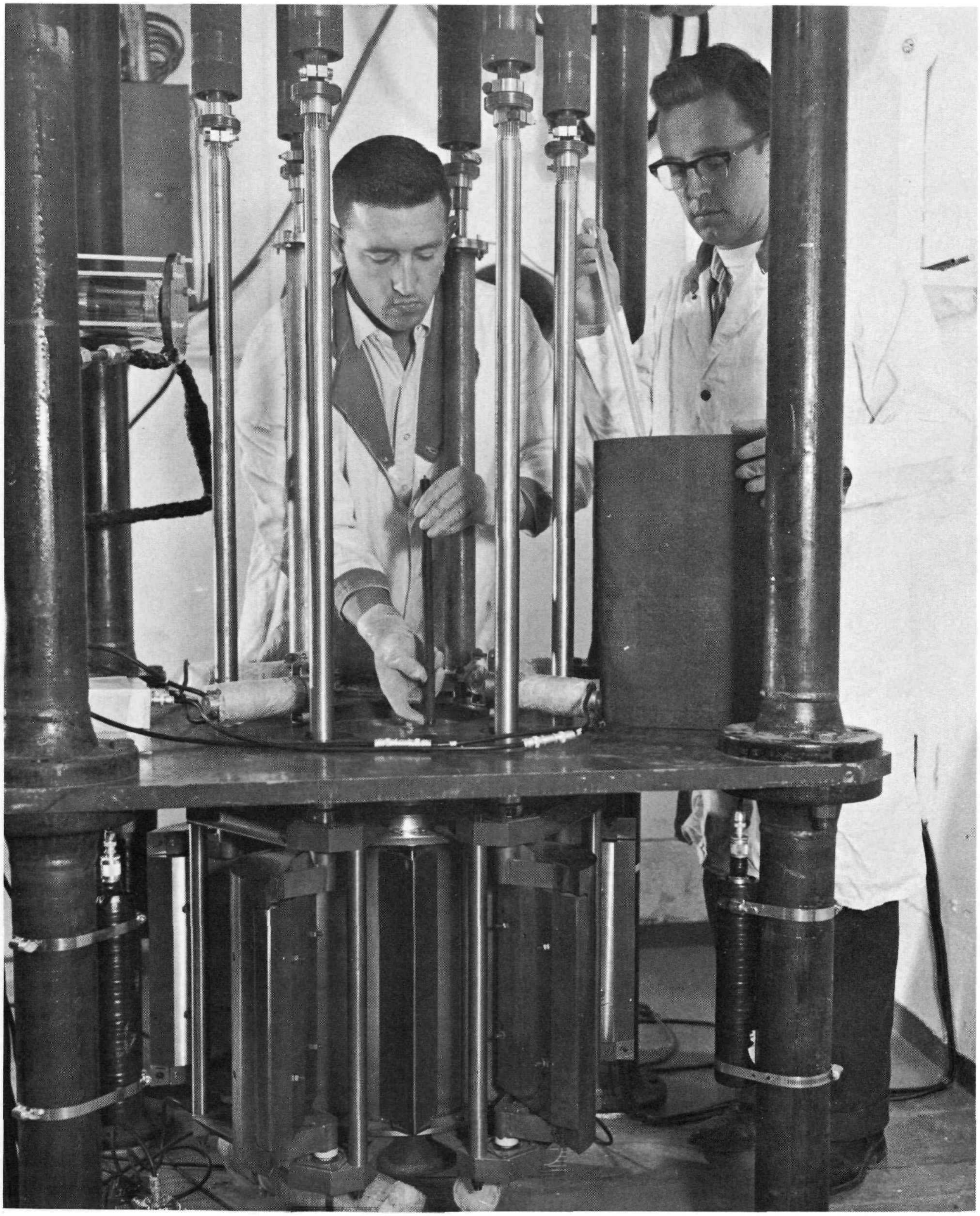

10-10-62 7568-5520

Figure 4. S8ER Critical Experiment Loading Operations

necessary to fulfill experimental and safeguards requirements. Essentially trouble-free performance of the critical machine was realized during the three months required for experimental operations. The principal experimental components, in addition to the core assembly, are the reactor vessel and reflector assembly, the reflector drive mechanisms, the nuclear instrumentation, and the neutron sources.

1. Reactor Vessel and Reflector Assembly

The reactor vessel is a thin-walled right circular cylinder (9.352 in. OD) which contains the core assembly and, for normal power operations, the NaK coolant. (No NaK was introduced during the "dry" critical experiments described herein.) The lower end of the vessel (inlet plenum) is a reverse dished head approximately four in. deep. The upper head (outlet plenum) consists of an open-ended cylindrical section about 3.5 in. long. The vessel mounting flange is welded to the upper end of this component, and a reflector support flange is welded to each vessel head section. Overall vessel height is approximately 24 in. The vessel used in these experiments was a duplicate of the power test vessel with the exception of the vessel mounting flange and outlet nozzle hardware on the upper head. Pertinent reactor data and dimensions are summarized in Table 1 and cross sectioned views of the reactor are shown in Figure 5.

The external beryllium reflector used to control reactivity consists of six, equally spaced, rotatable elements which are segments of a right circular cylinder. These six control "drums" almost completely surround the cylindrical portion of the reactor vessel as shown in Figure 5. Six triangular-shaped, stationary beryllium reflectors fill the small voids between the vessel and the rotatable elements. The reflector control assembly was fabricated in two halves. A photograph of the reactor vessel and reflector assembly is shown in Figure 6. In this view the reflector assembly halves are separated slightly to show the stationary reflectors, and the reflector support flanges.

Reactivity control is achieved by rotating the drums about their center of curvature and thereby adjusting the rate of neutron leakage from the core. The thickness of the control drums may be adjusted, prior to startup, by adding or removing shim material. These shims are identified in Figure 1 as shim A (negative) and shim B (positive). Figures 4, 5, and 6 show both the A and B shims installed. The nominal 3-in. effective reflector thickness is made up of

TABLE 1

S8ER CRITICAL EXPERIMENT CHARACTERISTICS

Reactor Vessel	
Material	316 SS
Outside diameter, in.	9.352
Wall thickness, in.	
Core region	0.0626
Lower head	1/8
Upper head	1/4
Approximate heights, in.	
Lower head	4
Upper head	3-1/2
Overall	24
External Reflectors	
Material	Be
Number of drums	6
Number of stationary pieces	6
Length, in.	14.5
Density, gm/cm^3	1.84
Drum radius of curvature, in.	4.68
Core vessel – reflector radial gap, in.	0.0818
Shim thickness, in.	
A	0.750
B	0.880
C	1.13
Shim length, in.	12
Effective reflector thickness, in.	
No shims	2.34
A shims	3.08
A + B shims	3.78
A + B + C shims	4.73
Normal Drum Rotation Range, °	105
IN position (maximum reactivity)	105
OUT position (minimum reactivity)	0
Fuel-Moderator Elements	
Number	211
Length (minus grid pins), in.	14.469 (average)
Outside diameter, in.	0.562 (average)
Weight, gm	367.0 (average)
Fuel Rods	
Material	enriched U-Zr alloy, Zr hydrided
Outside diameter, in.	0.532
Length, in.	14.0
Weight, gm	309.653 (average)
U total weight, gm	30.40 (average)
U^{235} enrichment, wt %	93.15 (average)
N_H, $atoms/cm^3$	5.96 (average)
Uranium, wt %	9.82
Zirconium, wt %	88.53
Hydrogen, wt %	1.65
H/Zr atom ratio	1.7
Fuel rod density, gm/cm^3	6.06
Fuel-to-Clad Gaps (0.1 atm. He at room temperature)	
Radial, in.	0.0016 (average)
Axial, in.	0.024 (average)

Cladding	
Material	Hastelloy-N
Outside diameter, in.	0.562 (average)
Wall thickness, in	0.0104 (average)
End cap thickness, in.	
Upper	0.08
Lower	0.37
Ceramic Coating	
Material	AI-8763D
Thickness, in.	0.0022 (average)
Burnable poison, Sm_2O_3, mg/in of clad	2.88
Core (Fueled Region, 211 Fuel Elements)	
Equilateral triangular lattice spacing, in.	0.570
Diameter across corners, in.	9.25
Diameter across flats, in.	9.0
Equivalent core diameter, in.	8.694
Core length, in.	14.0
Volume Fractions	
Fuel-moderator rods	0.790
Fuel void (He)	0.010
Cladding – Hastelloy-N	0.067
Ceramic coating	0.013
Void (NaK volume)	0.120
Total uranium, kg	6.44
Total SmO_3, gm	8.51
H/U^{235} atom ratio	42.4
Core – External Reflector Radial Interface	
Equivalent annular thickness, in.	0.382
Volume fractions	
BeO (Internal Reflectors)	0.410
Hastelloy-N	0.042
Stainless steel - 316	0.191
Void	0.357
Core Axial Structure	
Lower end cap thickness, in.	0.394
Volume fractions	
Hastelloy-N	0.737
Void	0.263
Lower grid thickness, in.	0.313
Volume fractions	
Hastelloy-C	0.830
Hastelloy-N	0.057
316 stainless steel	0.018
Void	0.095
Upper end cap thickness, in.	0.08
Volume fractions	
Hastelloy-N	0.851
Void	0.149
Upper grid thickness, in.	0.344
Volume fractions	
Hastelloy-N	0.031
316 stainless steel	0.794
Void	0.175

*Average value denotes as-built inspection results. See Reference 3.

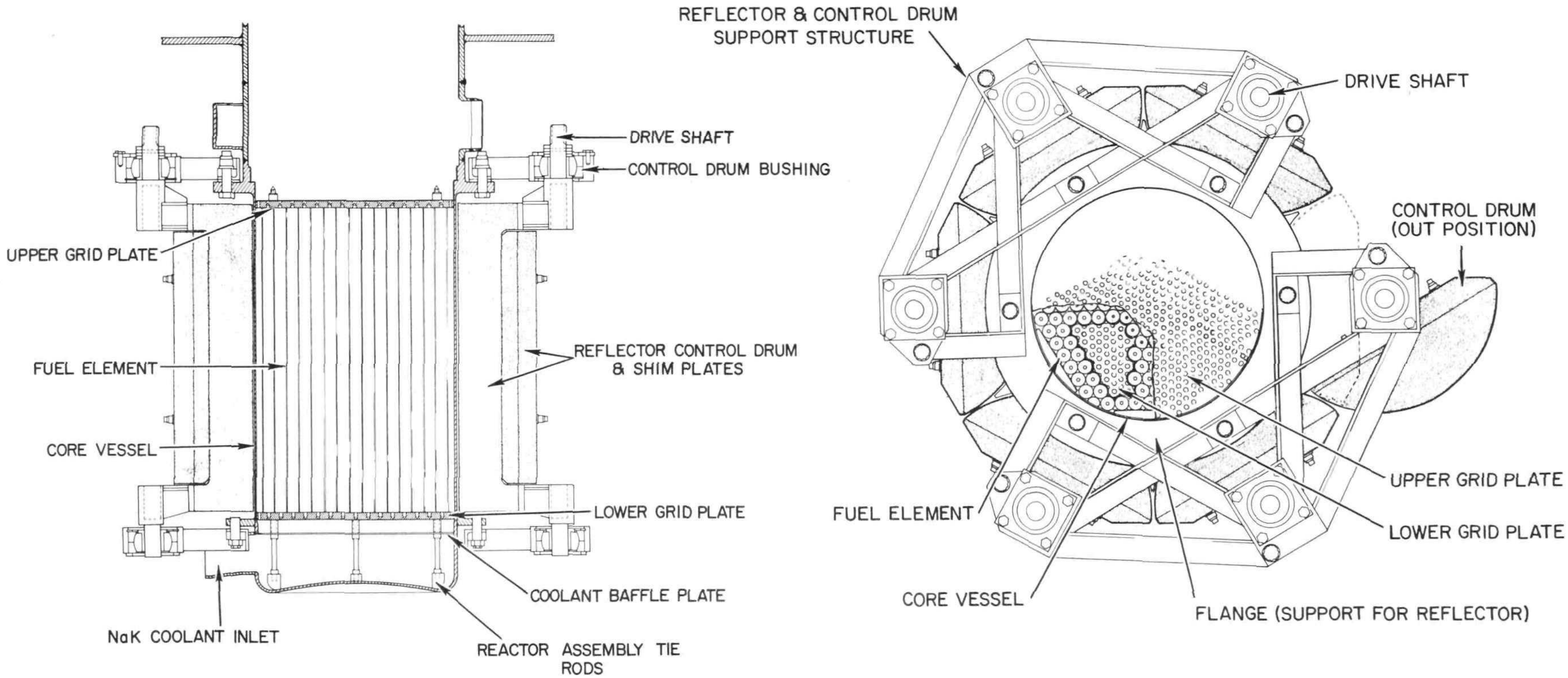

8-11-64 7570-80118C

Figure 5. S8ER Assembly

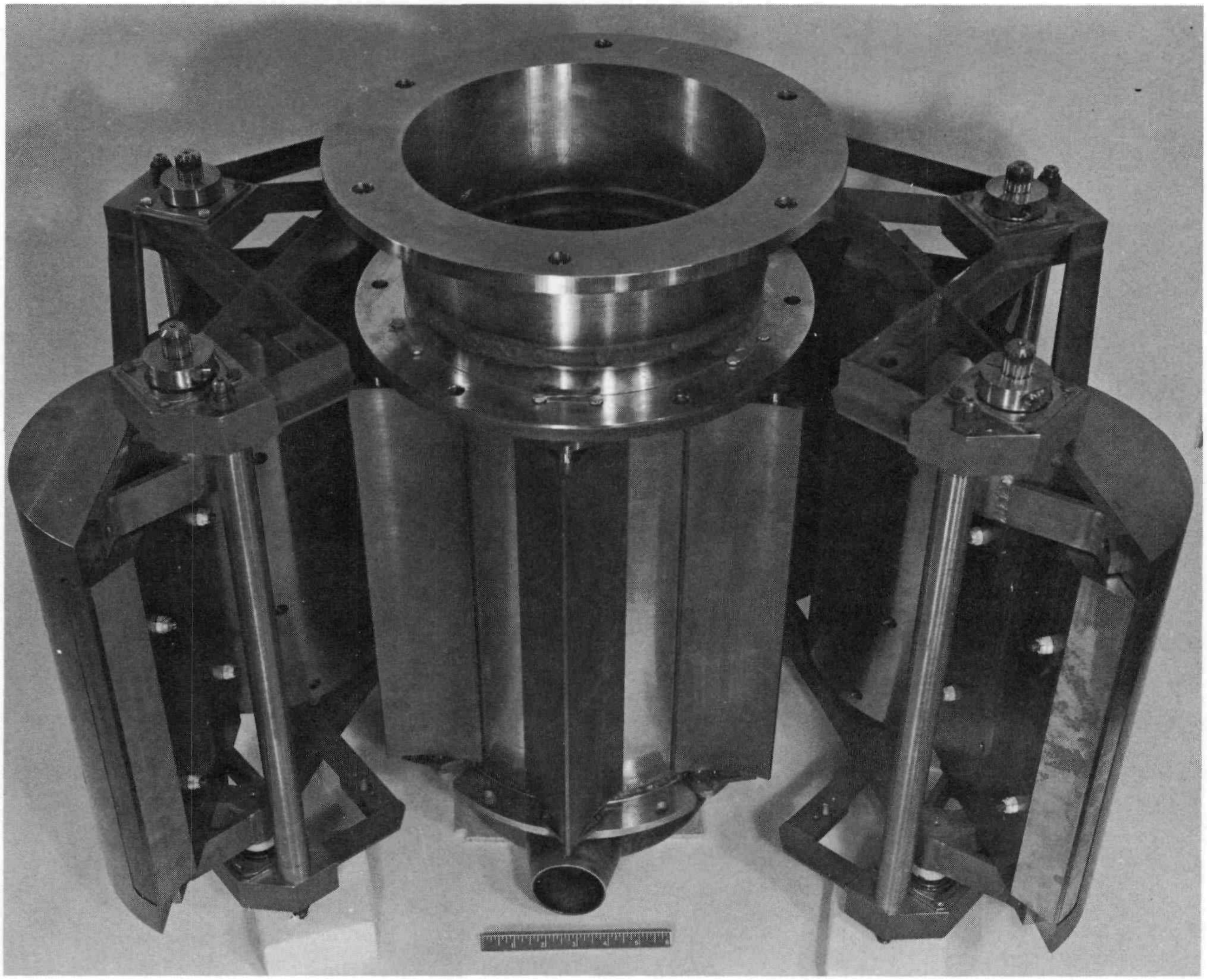

5-24-62 7570-5208B

Figure 6. S8ER Critical Reactor Vessel and Reflector Assembly
(Reflector assembly halves slightly separated)

the six control elements, with the A shims attached, and the six stationary reflector pieces. Additional reactivity may be added to the system if required, by the B shims. Likewise the system reactivity may be reduced by removal of the A shims.

To provide additional information on the relationship of reactivity to effective reflector thickness, a single C shim was installed between the A and B shim of one drum for some of the experiments.

The axial "reflectors" consist of the core structural hardware at the ends of the fuel and the NaK coolant, when it is present. Internal reflectors are described in Section II-B.

2. Reflector Drive Mechanisms

Each of the six control drums has an independent drive mechanism to provide both position and safety functions. A reversible a-c motor is connected to the drum-drive linkage through a worm gear and an electromagnetic rotary scram clutch. Scram energy is stored in a spiral torsion spring loaded to rotate the drum to the full-out position when the clutch is deenergized. When the clutch is energized, the entire drive linkage including the drum position sensors is torsionally rigid and the force of the scram spring on the linkage eliminates backlash. The direct coupling provides an accurate drum position indication for the two position indication systems. The coarse system indicates drum positions to ±0.5°, and the fine system has an overall accuracy of ±0.07°.

For normal reactivity control, only one drum can be positioned at a time. Rotation of a drum from full-out (0°) to full-in (105°) requires 319 sec. Scram action will cause all drums to rotate-out simultaneously with a total scram time of less than 0.490 sec.

The excess reactivity available to the operator was restricted during these experiments. Lockout brackets were used as required on all six drive shafts. Stops at intermediate drum positions were also provided for drum calibration measurements.

Sections of two of the drive shafts were mounted with quick-disconnect couplings to facilitate access to the reactor core.

3. Nuclear Instrumentation

The Instrumentation and Safety System is essentially identical to those used in previous experiments in this facility. For experimental purposes, four fission counter channels and two ion chamber channels were monitored. Fission counter measurements were obtained in terms of scaler-timer readouts, log and linear count rate indications. Ion chamber signals were displayed directly and were printed as successive counts using a voltage-to-frequency converter, counter, and printer arrangement. Figure 4 shows the detector locations. The fission counters are installed on the four legs of the critical machine and the ion-chambers are placed beneath the core. Four neutron scintillation counters are shown around the opening in the core support table. These detectors supplied signals to the multi-channel time analyzer for pulsed neutron experiments and to specialized recording equipment for subsequent pile noise analysis. Reference 2 describes the experimental and analytical techniques for the noise measurements.

4. Neutron Sources

A Pu-Be source of 2×10^6 n/s was adequate for subcritical monitoring of reactor power. For pulsed neutron experiments a linear-accelerator pulsed neutron source was provided.

B. REACTOR CORE ASSEMBLY

The S8ER core is comprised of 211 fuel-moderator elements and 18 internal reflector inserts. These components are fitted at each end with grid plate indexing pins that engage holes in the upper and lower grid plates to provide the required support and spacing. In turn, the grid plates are supported and spaced within the reactor vessel by six axial tie rods evenly spaced around the circumference of the core. Figure 7 is a photograph looking down on a partially

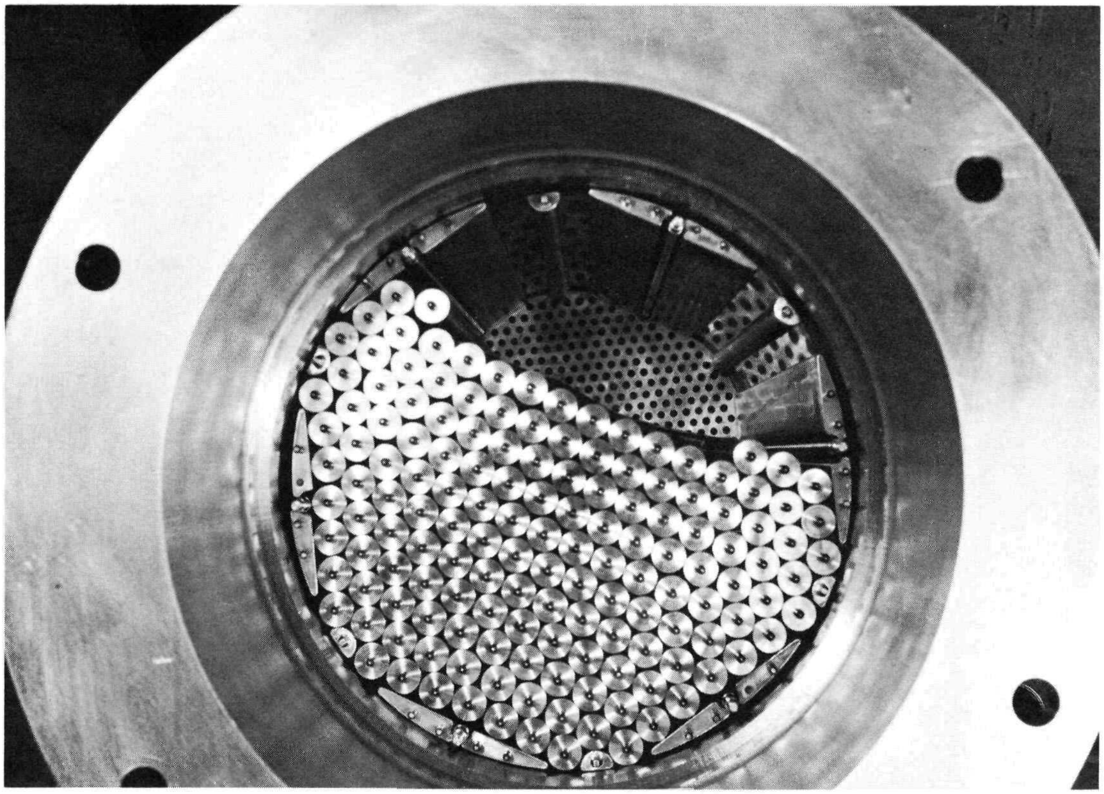

4-4-62 7570-5207C

Figure 7. SNAP 8 Core Mockup

fueled mockup with the upper grid plate removed and a portion of the lower grid plate exposed at the base of the core. The fuel outline is a regular hexagon with the fuel elements at the six corners of the array replaced by D-shaped internal reflector inserts. The segment volume between the reactor vessel and each hexagonal flat boundary of the fuel array is filled with two airfoil-shaped reflector inserts on either side of a tie rod. Additional data are presented in Table 1 and the paragraphs below.

1. Fuel-Moderator Elements

An S8ER fuel element is illustrated in Figure 8. The fuel rod is a right circular cylinder formed of a fully enriched uranium-zirconium alloy that is hydrided to an average N_H of 5.96 x 10^{22} atoms/cm^3 of fuel. This atom density of the hydrogen moderator is only slightly less than the hydrogen density in water. Thus, the U^{235} fuel and the hydrogen moderator are uniformly distributed throughout the fuel rod.

The fuel-moderator rods are clad with Hastelloy-N tubing (0.560-in.-OD x 0.010-in.-wall) and end plugs. The inside of the tubing is coated with a ceramic hydrogen barrier material to minimize hydrogen leakage from the fuel under design operating conditions. Sealing the final assembly consists of blending the coating on the lower end plug with that on the tubing and seal welding the plug to the tubing. The coating on the tubing and upper end plug also contains a burnable neutron poison (Sm_2O_3), while the coating on the lower end plug contains none. Finished fuel elements are qualification tested for an acceptably low hydrogen leak rate. Those elements not acceptable are rejected as "unqualified." Although these elements are not suitable for power production, they are nuclear duplicates of their qualified counterparts at room temperatures. Several unqualified elements were used to permit these experiments to be initiated prior to completion of a full, qualified array of S8ER elements.

The S8ER fuel-moderator array is shown in Figure 9. Elements are spaced on a 0.570-in. uniform equilateral triangular grid. Individual elements are identified by ring number (Roman numerals I through IX) and a position number in the ring (arabic numerals).

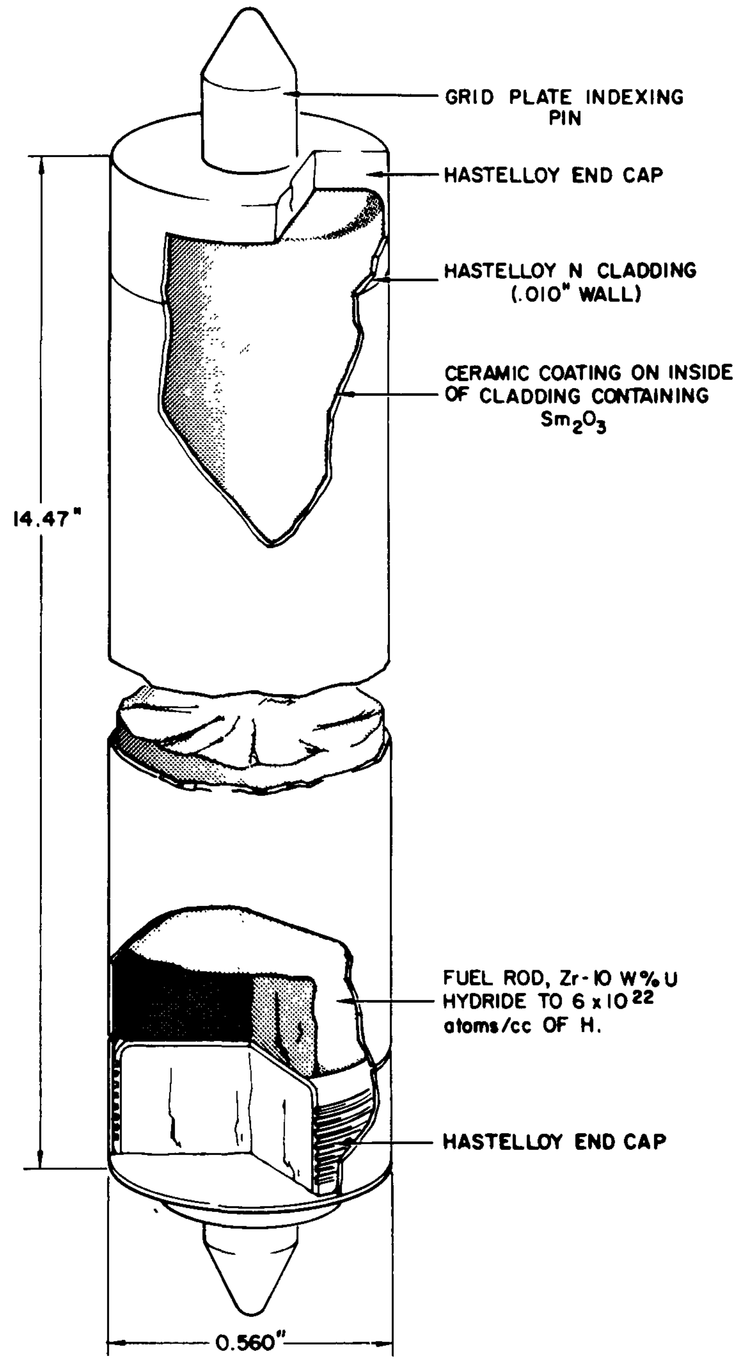

8-19-64 7568-01490

Figure 8. S8ER Fuel Element

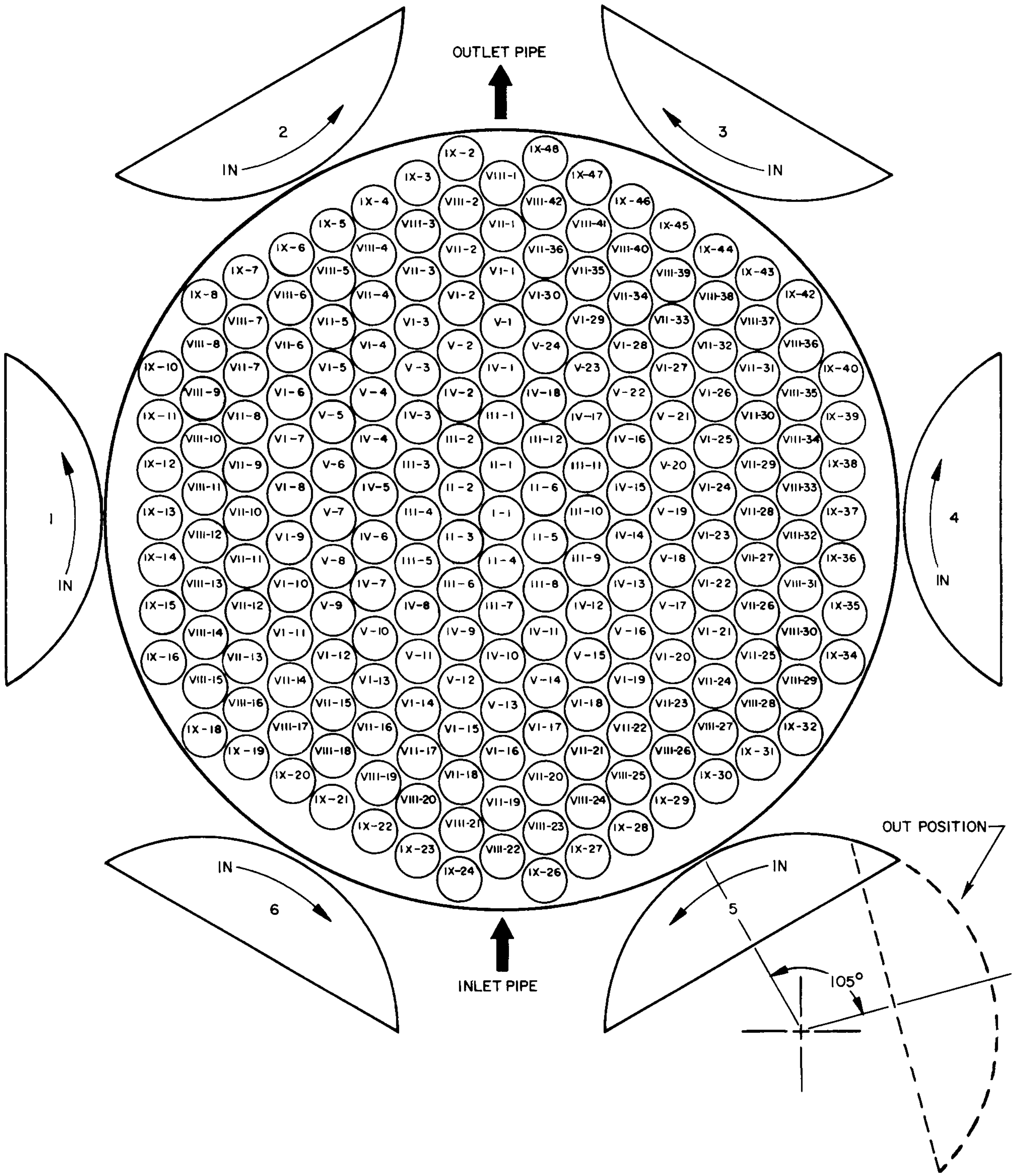

8-7-64 7568-01474

Figure 9. Fuel and Drum Array

2. Internal Reflectors

Internal reflectors occupy the space on the periphery of the core between the hexagonal-fuel-element pattern and the cylindrical reactor-vessel shell. These internal reflectors are made of a BeO hot-pressed to 98% of theoretical density and clad with 0.010-in.-thick Hastelloy-N. They extend the full length of the core between the upper and lower grid plates.

3. Structural Hardware

The upper and lower grid plates are circular discs 9-3/16 in. in diameter. The lower grid is made of Hastelloy-C plate, 5/16 in. thick; the upper grid is made of Type 316 stainless steel plate, 11/32 in. thick. Both grid plates are pierced by 211 holes 9/64 in. in diameter in a triangular array to position and hold the fuel elements in the core. In addition to these fuel-element-positioning holes, both grid plates are pierced by 420 coolant flow holes arranged in a hexagonal array superimposed on the fuel array. In the upper grid, the coolant flow holes are 5/32 in. in diameter, while in the lower grid they are 1/8 in. Thirty 1/8-in.-diameter holes are located on the periphery of both grid plates to position and hold the 18 internal reflectors. Six more peripheral holes accommodate the tie rods.

The core tie rods are 7/32-in.–OD Type 316 stainless steel. They bear on the base of the reactor vessel and support the core within the vessel as shown in Figure 5.

A coolant flow baffle plate is located in the lower plenum of the reactor vessel 5/8 in. below the lower grid plate. This baffle is a 9-3/16-in.-diameter disc of 316 stainless steel, 1/16 in. thick.

C. EXPERIMENTAL TECHNIQUES AND LIMITATIONS

Reactivity adjustments were made by: (1) changing the fuel loading; (2) changing the control drum shim configurations; (3) changing control drum positions; and (4) introducing and removing special elements and materials of various moderating, capturing, and fissioning capabilities. At all times, the excess reactivity available to the operator for supercritical measurements was physically limited to less than 50¢. This was achieved by locking a drum in the OUT position and/or restricting the rotation of one or more drums with intermediate stops.

The excess reactivity of a particular assembly was measured in terms of the stable reactor period. The period was obtained from semilog plots or least-squares fitting of the indication vs time from at least two nuclear instrumentation channels. Conventional inhour relationships were used to convert the period to reactivity in cents. An effective delayed neutron fraction of 0.0077 was used to convert dollars to reactivity ($\Delta k/k$).

Subcritical reactivity additions were monitored in terms of inverse multiplication (1/n) plots vs either the number of fuel elements added or angle of drum insertion. Incremental fuel additions were limited to no more than half of the elements required to achieve criticality (based on the spatial average of the extrapolated 1/n plots) provided the contained U^{235} was no greater than 400 gm (12 elements). When criticality was extrapolated to within two elements, only one fuel element was added at each step. In a similar fashion, drum reactivity additions near critical were limited by 1/n extrapolations to produce a positive stable period of 20 sec or more.

Attempts to directly measure subcritical reactivities by pulsed neutron and "rod-drop" techniques were unsuccessful. The available pulsed neutron generator could not be positioned close enough to the core to produce a satisfactory yield of fission neutrons for the decay measurement. The reactivity increments associated with the rod-drop experiments were sufficiently large (> $3) that the "prompt jump" could not be resolved with the equipment available at the time of the experiments.

All of the measurements were obtained with the assembly at an essentially constant room temperature (~ 75°F). No reactivity variations were observed that could be attributed to temperature variations.

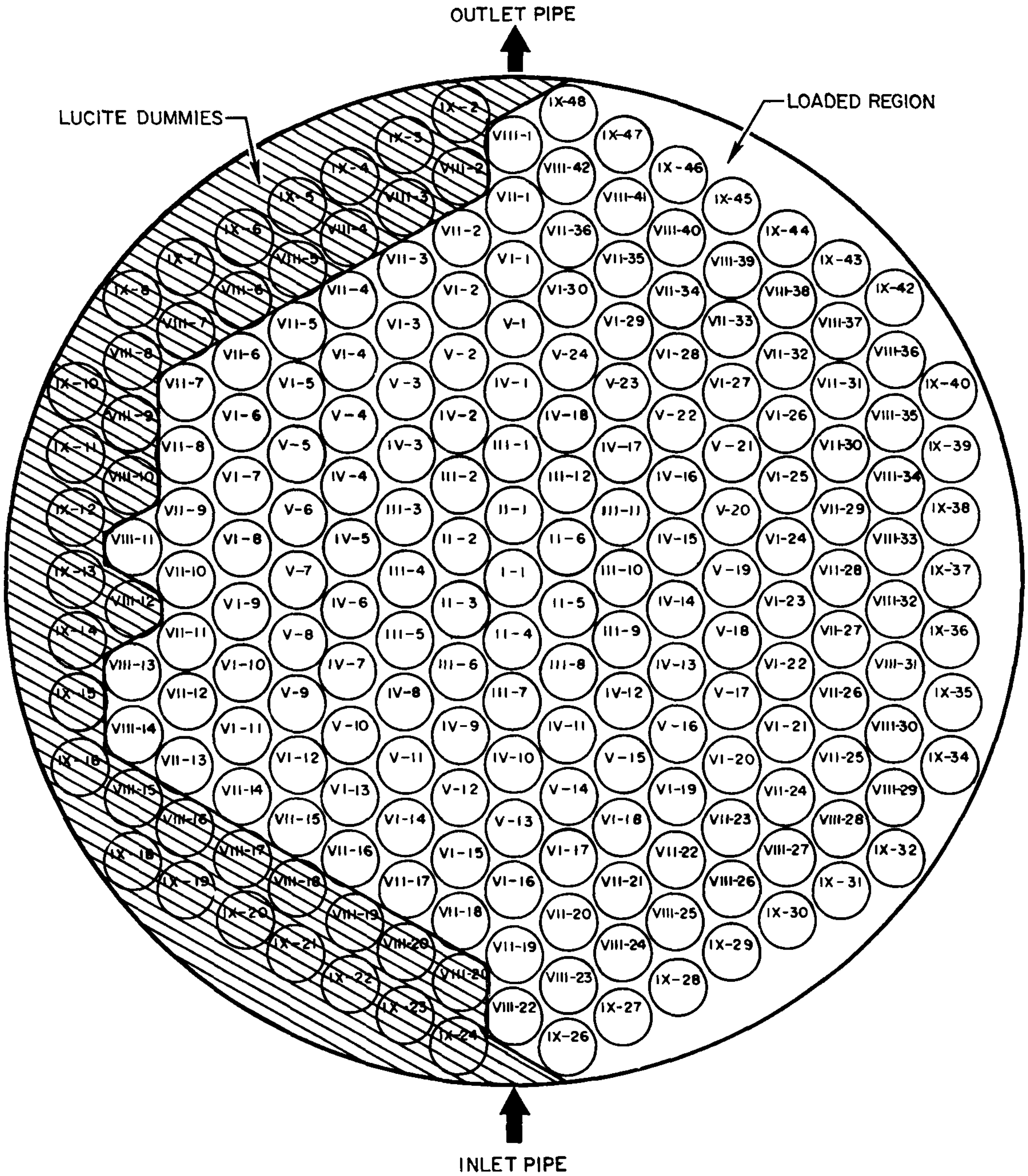

8-7-64 7568-01475

Figure 10. Initial Critical Loading – A and B Shims

III. MEASUREMENTS AND RESULTS

The initial loading approach to critical was begun with the 211 dummy lucite rods in the fuel-moderator positions and a complete array of internal reflectors. Lucite rods were replaced with fuel-moderator elements as the loading was increased. Reductions in loadings were accomplished by reversing the process and substituting lucite for fuel. Thus, all core positions were filled with normal, test, or dummy components during all measurements excepting void worth determinations.

The core was loaded starting from one side of the core and working toward the other. The resultant critical loadings were somewhat skewed hexagonal cylinders whose vertical axes were displaced slightly from the axis of the core vessel. Partially fueled critical loadings generally contained a crescent-like lucite region between one side of the fuel-moderator and the reflector similar to that shown in Figure 10. This loading sequence was required to assure positive coupling between the "uncontrolled" fuel-moderator region and the external reflector where the control elements are located.

These general core loading conditions prevailed throughout the testing described below.

A. CRITICAL LOADINGS

Initial criticality of the S8ER assembly was achieved on September 17, 1962, with the A and B reflector shims installed. The critical array is shown in Figure 10 and the core conditions are summarized in Table 2 under critical loading C-1. Figure 11 shows the tail of the inverse multiplication vs number of fuel elements plot of two typical channels for this loading. All channels extrapolated to a critical loading of 172.2 ± 0.1 fuel-moderator elements.

Subsequent critical loadings with different shim or drum configurations are also described in Table 2. As expected, the number of fuel-moderator elements required to obtain criticality increased as the effective reflector thickness was reduced. However, the experimentally determined critical loadings were larger than those predicted using the FAIM diffusion code.[4]

The calculational error shown in Table 2 is the reactivity difference between the theoretical reactivities obtained for the calculated and measured

TABLE 2

S8ER CRITICAL LOADINGS

	Loading Designation			
	C-1	C-2	C-3	C-4
Shims installed	A-B	A	None	A-B
Effective reflector thickness, in.	3.78	3.08	2.34	3.78
Drums locked out	None	None	None	No. 6
Number lucite rods	38	25	0	20
Number fuel-moderator elements	178	186	211	191
Excess reactivity, ¢	+9.7	+14.3	-28*	+9.3†
Extrapolated critical loading	172.2	185.4	213.2	190.2
Calculated critical loading	152	169	196	---
Calculational error, %Δk/k	3.0	2.0	1.5	---

*Criticality was not achieved with the fully loaded core. Negative reactivity was estimated from extrapolated critical loading.

†Excess available to operator if Drum No. 6 were unlocked would have been 374¢.

critical loadings. It appears that the error is sensitive to reflector thickness. This sensitivity is probably exaggerated because the one-dimensional FAIM model cannot totally describe the physical asymmetries of the experiments involving less than 211 fuel-moderator elements. Although FAIM had proved remarkably successful in predicting the excess reactivities of previous SNAP reactor assemblies, experiment and theory did not closely agree in this case. It is believed that the discrepancy is due to limitations imposed by (1) a relatively small number of thermal neutron energy groups, (2) one-dimensional geometry approximations, and (3) the normal diffusion theory approximations. After-the-fact calculations of the excess reactivity using more sophisticated diffusion or transport theory approaches have reduced the errors to less than 1% (Δk/k).

Critical loading C-4 was the reference core condition for measurements of power distributions and the worths of special fuel rods and absorbers. With this configuration, the excess reactivity could be conveniently increased or decreased in small increments to measure the reactivity changes produced by special materials. Also, at the core positions where the reactivity effects were measured, the reactor response was effectively that of a fully fueled core.

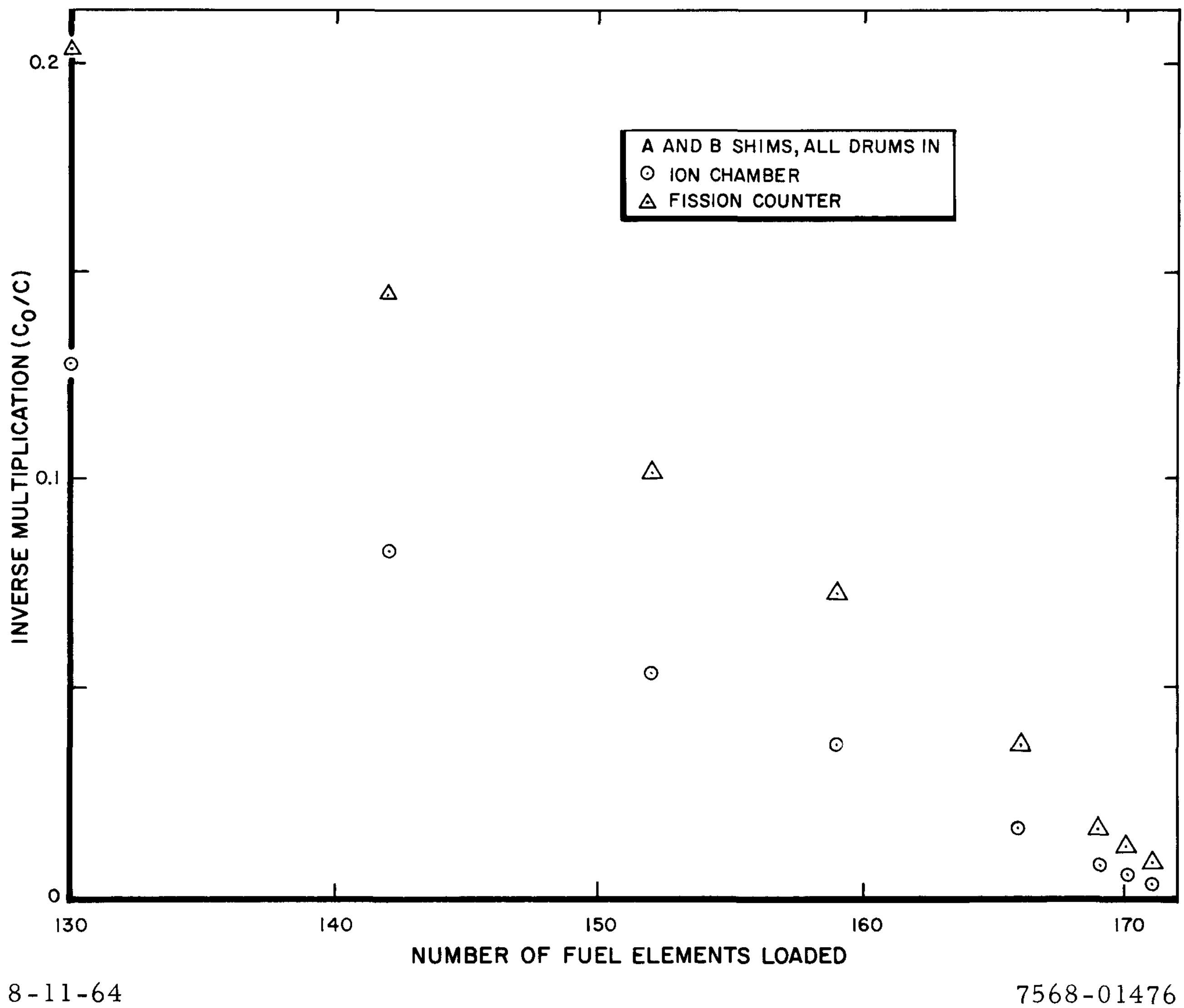

Figure 11. Initial Approach to Critical Loading

B. RADIAL REFLECTOR WORTH

The incremental reactivity worths of four reflector shim configurations (or effective radial reflector thicknesses) were determined. Comparative results are shown in Table 3.

B shim worth was determined by measuring a reactivity loss of 46¢ due to the removal of a single B shim from Drum No. 3 with A and B shims on all other drums. The worth of B-shim configuration was obtained by multiplying the single shim worth by six. This assumption that the single B-shim worth is representative of the average is not completely rigorous. However, it does

TABLE 3

RADIAL REFLECTOR WORTH

	Effective Reflector Thickness (in.)				
	2.34	3.08	3.78	4.73	4.47
Shim configuration	None	A	A-B	A-C-B	A-B-B
Shim measured		A	B	C	Second B
Actual shim thickness, in.		0.75	0.88	1.13	0.88
Effective shim thickness, in.		0.74	0.70	0.95	0.69
Single shim worth, ¢		58.7	46	41	28.5
Six-shim worth, $		3.52	2.76	2.46	1.71
Six-shim worth, %Δk/k		2.71	2.13	1.89	1.32
Predicted six-shim worth, %Δk/k		3.0	2.5	Not Predicted	

provide an evaluation that is within the limits of uncertainty of the only relatively elegant and expensive calculational techniques available.

For the A shims, the total worth was deduced by subtracting B shim worth from the difference between the excess reactivities determined for the no-shims and A-B shims configurations (see Sec. III-H). The single A shim worth of 58.7¢ listed in Table 3 is one-sixth of the total.

The critical loading determinations pointed up the possible need for increased effective reflector thickness to provide sufficient excess reactivity for core lifetime requirements. Two single-shim worth measurements were obtained using methods similar to the B shim worth determinations above. A second B shim (previously removed from Drum No. 1) was added to Drum No. 3 and a reactivity gain of 28.5¢ was measured. The extra thickness of two B shims on Drum No. 3 prevented it from being rotated to the full-in (105°) position because of mechanical interference from the adjacent structural tie rod. There is one such rod between the upper and lower reflector assembly frames adjacent to each set of drum bearings (see Figure 6 for example). The reactivity measurement was made with Drum No. 3 at 85.83°. From a consideration of the drum calibration measurements, the worth of the second B shim at 85.83° is effectively the same as at 105°. The C shim, installed between the A and B shims of Drum No. 4 (which could be rotated in to 105°), added 41¢. As in the initial

B shim measurement, the incremental worths of the second B shim and the C shim configurations were obtained by multiplying the single shim worths by six.

The predicted shim worths listed in Table 3 were obtained with the aid of ULCER[5] — a 40-group, one-dimensional diffusion theory code. This code provides a more refined definition than FAIM of the spatial thermal spectrum variation effects that are important when the reflector thickness is varied. In spite of these refinements, the error in reflector reactivity worths appears to increase with increasing reflector thickness as did the error resulting from the FAIM calculations of critical loadings in Section III-A above. The radial reactor model employed for both the FAIM and ULCER calculations was based on as-built dimensions and compositions where they were available. However, direct measurements of the density of, and impurities in, the Be reflector are lacking.

Measurements obtained from other beryllium plates fabricated by the S8ER vendor to S8ER specifications has revealed a potential calculated decrease in reflector worth of approximately 0.5% $\Delta k/k$. These differences between the assumed and the deduced "as-built" reflector density and impurities appear to account for the discrepancy between the calculated and experimental reflector worths.

C. CONTROL ELEMENT CALIBRATIONS

Control element or drum calibrations were obtained with three different shim configurations and with a variety of drum configurations to determine drum interactions. No calibrations of the bare, unshimmed drums were made because there was not sufficient reactivity to operate in this mode. Within the reactivity limits — both total and operational — the effects of reflector thickness and drum interactions were determined.

1. Effects of Reflector Thickness

Control Drum No. 5 was calibrated with an A shim and with an A-B shim configuration on all drums. The positions of the adjacent drums (Nos. 4 and 6) were maintained constant at the IN limit during the calibrations. Figures 12 and 13 show the drum worths obtained. A third calibration, shown in Figure 14, was made with an A-C-B shim configuration on one drum and A-B shims on the remaining five drums. Measurements of the A shim and A-C-B shim included

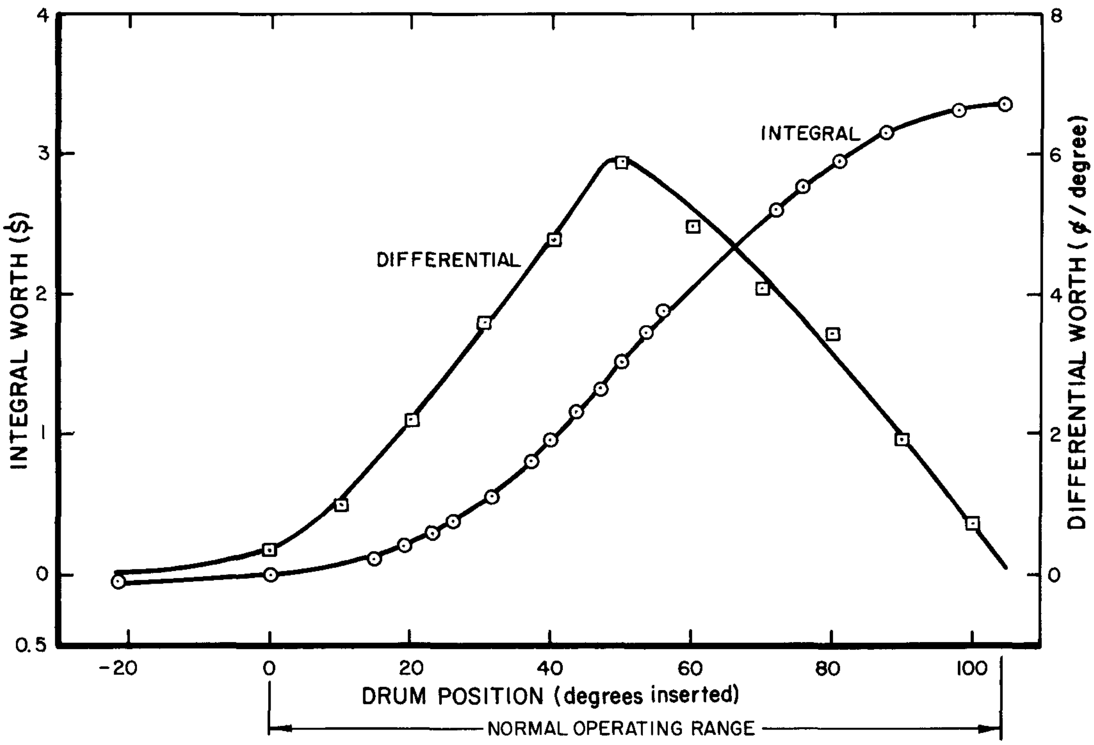

8-11-64 7568-01477

Figure 12. S8ER Control Element Worth — Drum No. 5 with A Shim

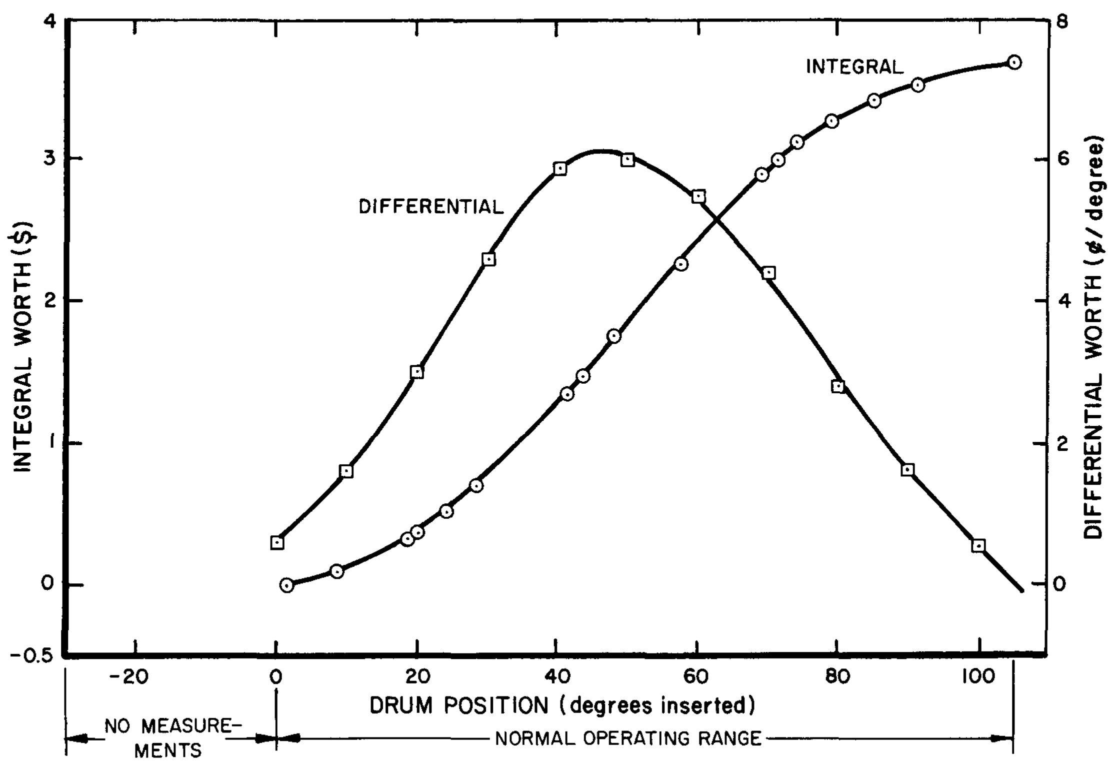

8-11-64 7568-01478

Figure 13. S8ER Control Element Worth — Drum No. 5 with A-B Shim

drum rotation about 22° beyond the normal OUT position of 0°. The drum worths as a function of reflector thickness are compared in Table 4.

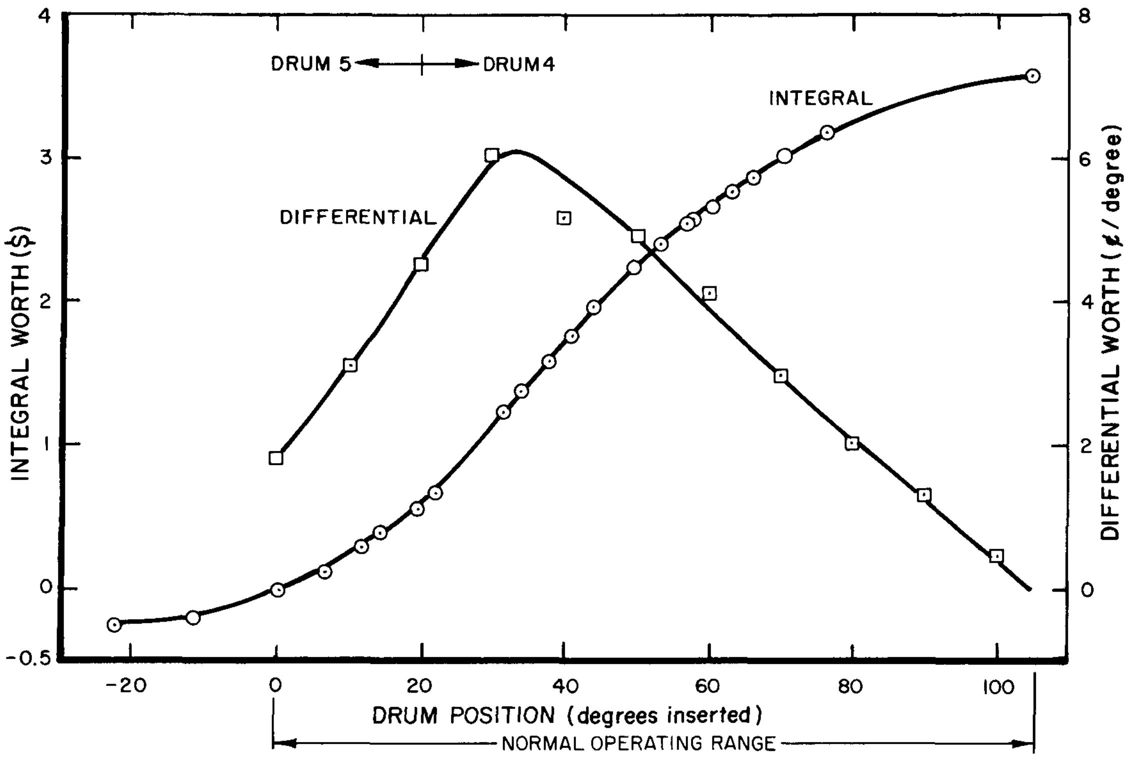

Figure 14. S8ER Control Element Worth – Drums Nos. 4 and 5 with A-C-B Shim

TABLE 4

CONTROL DRUM WORTH

	Effective Reflector Thickness (in.)		
	3.08	3.78	4.73
Shim configuration	A	A-B	A-C-B
Drum worths, $			
0° to 105°	3.37	3.67	3.56
-22° to 0°	0.04	---	0.24
Drum worths, %Δk/k			
0° to 105°	2.59	2.83	2.75
-22° to 0°	0.0308	---	0.185
Maximum differential worth, ¢/°	5.9	6.0	6.0

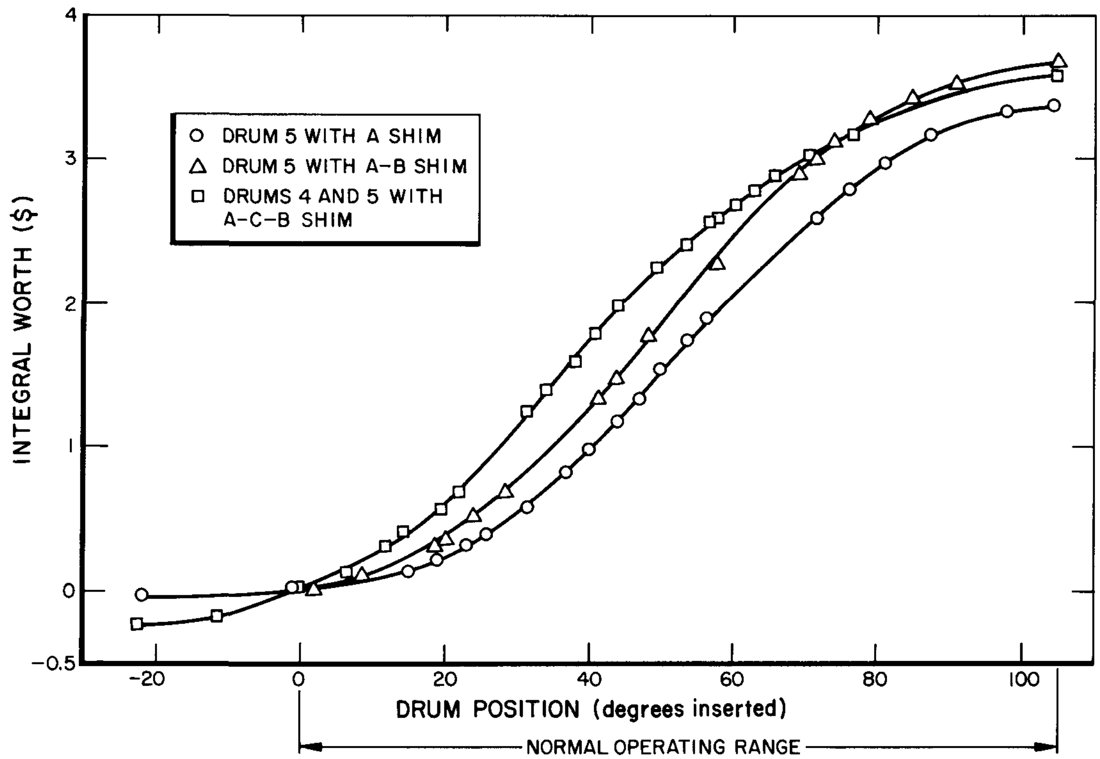

8-11-64 7568-01480

Figure 15. Total Integral Worth of S8ER Control Elements

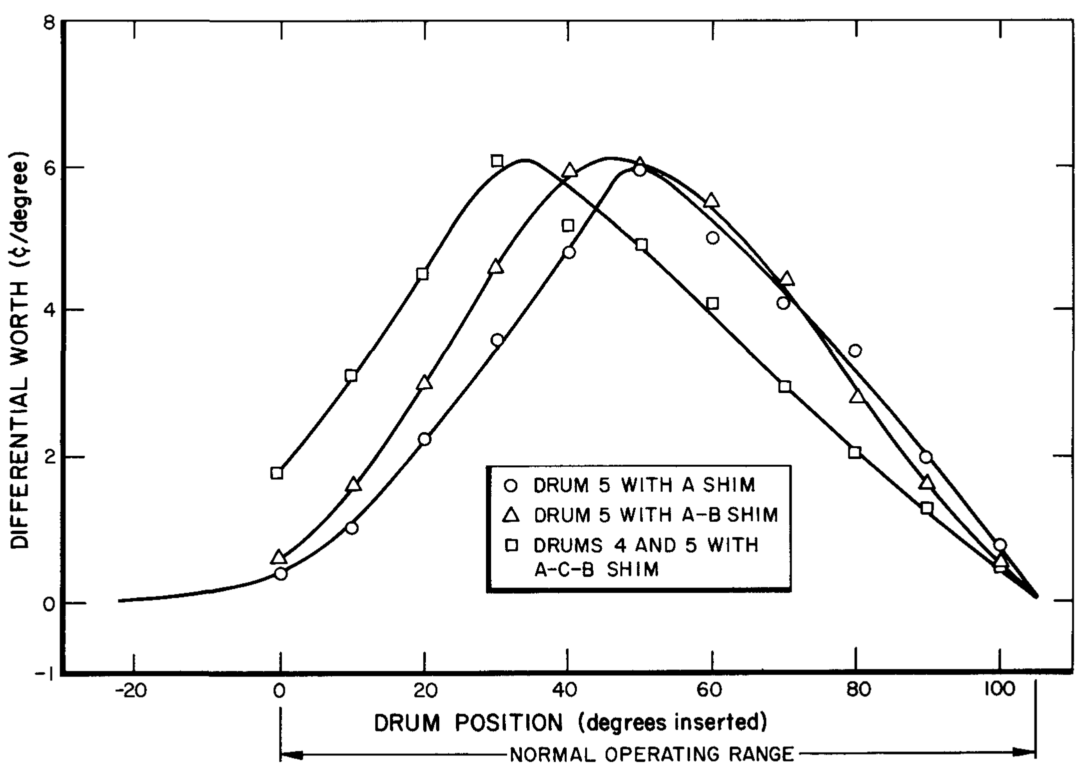

8-11-64 7568-01481

Figure 16. Differential Worth of S8ER Control Elements

The calibration curves in Figures 12, 13, and 14 were developed by traditional techniques. Stable reactor periods — produced by incremental rotations of the drum being calibrated — were measured and related to reactivity through the inhour formula. Compensating reactivity adjustments were achieved using other drums and/or by adjusting the fuel loading within the 50-cent excess reactivity limit imposed on the experiments. These adjustments were made in core regions remote from the drum being calibrated thereby minimizing — if not eliminating — any potential reactivity interaction effects. The incremental integral measurements were fitted and smoothed piecewise to construct the integral worth curves, and the differential worth curves were obtained graphically from the integral curves. An estimated maximum uncertainty of ±10 per cent in total worth is assigned to the calibrations.

Because of the symmetries associated with the measurements, i.e., adjacent drums IN, the calibrations obtained are assumed to be valid for any drum in a similar configuration. On this basis, the A-C-B shim calibration in Figure 14 was obtained using Drum No. 5 from -22° to +15° and Drum No. 4 from 18° to 105°. The mechanical interference of the structural tie rods prevented the use of a single drum over the entire range of drum rotation (see also Section II-B).

For comparison, the integral curves from Figures 12, 13, and 14 are presented in Figure 15 to show the effects of reflector thickness. A similar comparison is shown in Figure 16 for the differential worth.

The total worth of the A-shimmed drum was previously calculated to be 2.7% $\Delta k/k$, which compares favorably with the measured worth of 2.59%. A two-dimensional transport calculation was employed, using the 2DXY code with four-group cross sections.

2. Element Interactions

The worth of a control drum is expected to be dependent upon the core relative flux shape produced by the positions of the other drums. This interaction effect is quite pronounced between adjacent drums, particularly when these drums drive in toward each other as do Drums Nos. 5 and 6 or Drums Nos. 2 and 3 (see Figure 9). The worth of Drum No. 5 between the 70° and the IN position was measured with three different drum configurations and an A-B shim configuration. As shown in Figure 17, the worth of Drum No. 5 is not

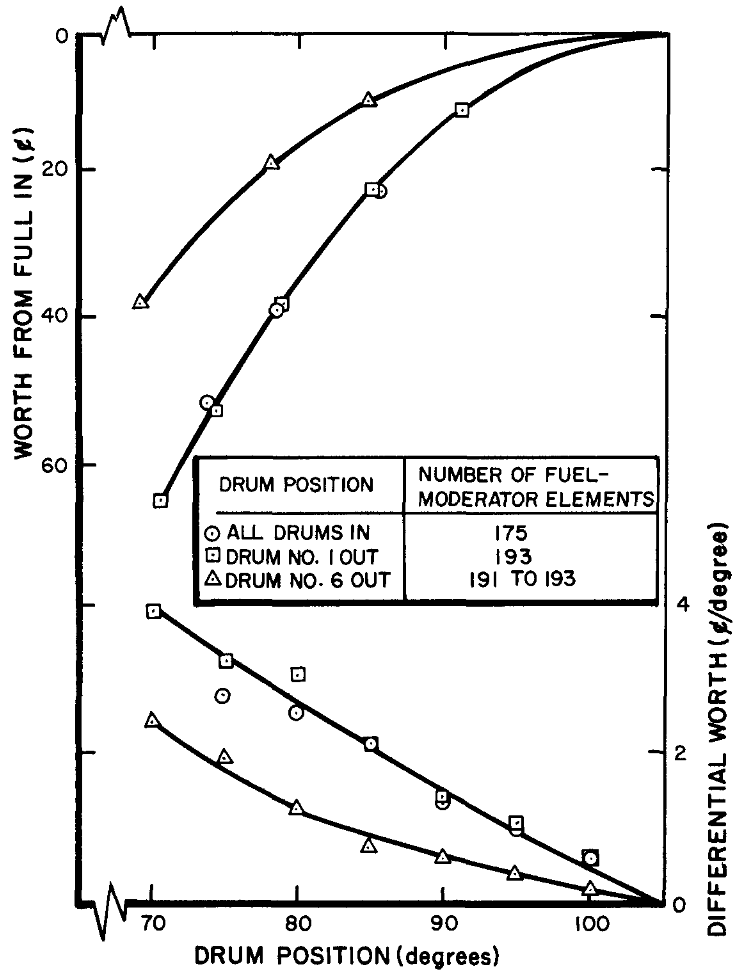

8-11-64 7568-01482

Figure 17. S8ER Control Element Interaction

significantly influenced by the position of Drum No. 1. However, the worth of the innermost 35° of Drum No. 5 is reduced by almost one-half when the adjacent Drum No. 6 is OUT.

D. POWER DISTRIBUTIONS

Axial and radial power distributions are shown in Figures 18 and 19. The experimental results are indicated by data points and are normalized to the calculated peak power at the center of the core. FAIM[4] and ULCER[5] codes were used respectively to obtain the calculated axial and radial power profiles.

The axial distribution was measured using a special fuel element at the core center position. The fuel-moderator rod consisted of seven two-inch segments which, with the exception of the uppermost segment, had essentially normal

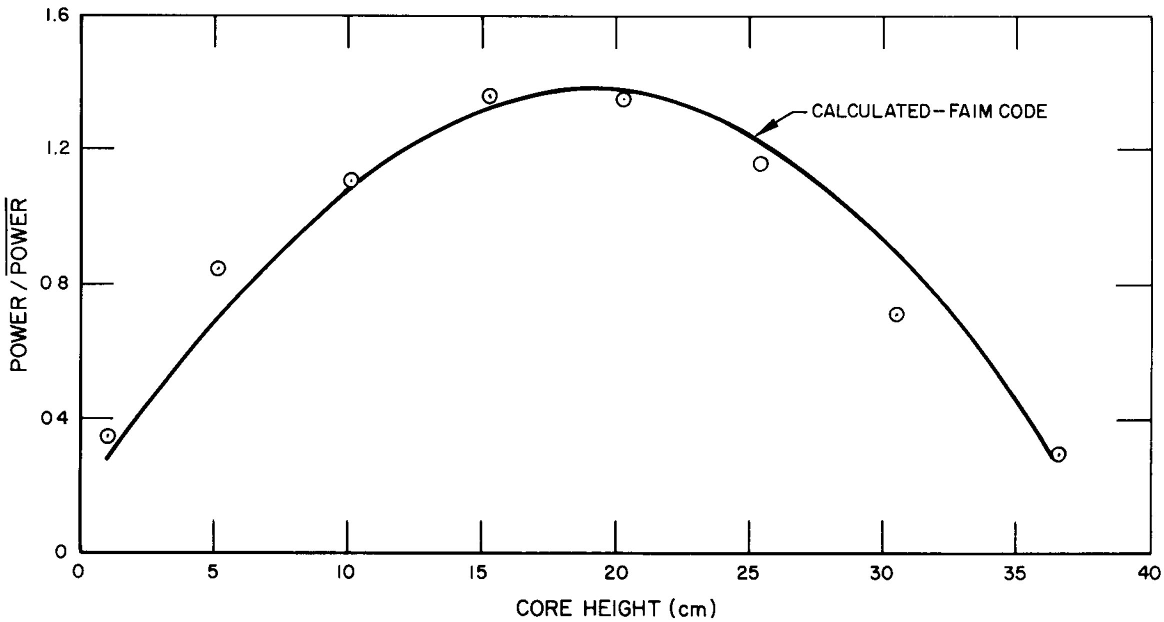

8-7-64 7568-4612

Figure 18. S8ER Axial Power Distribution

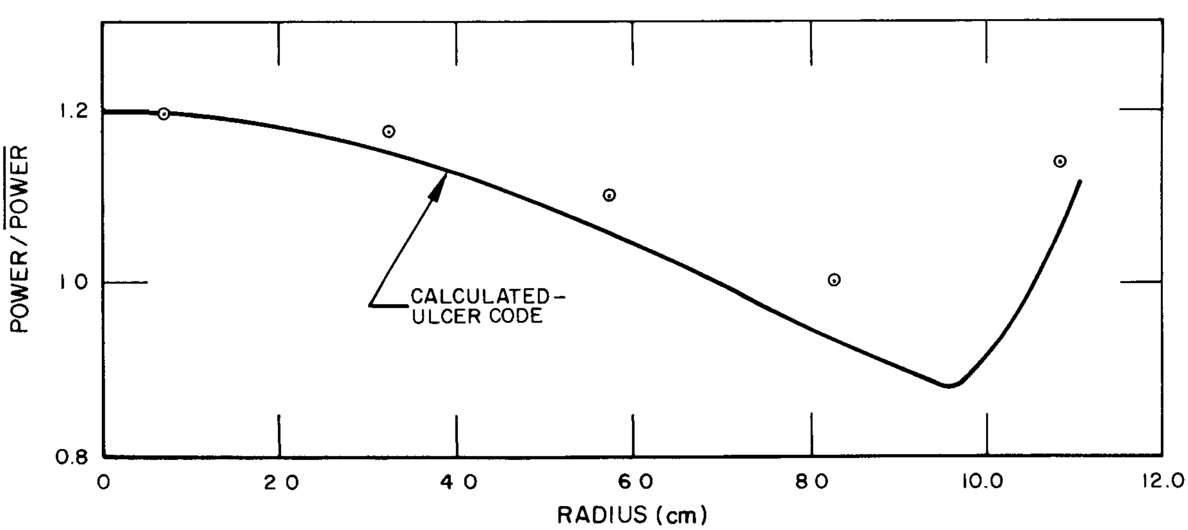

8-7-64 7568-4613

Figure 19. S8ER Radial Power Distribution

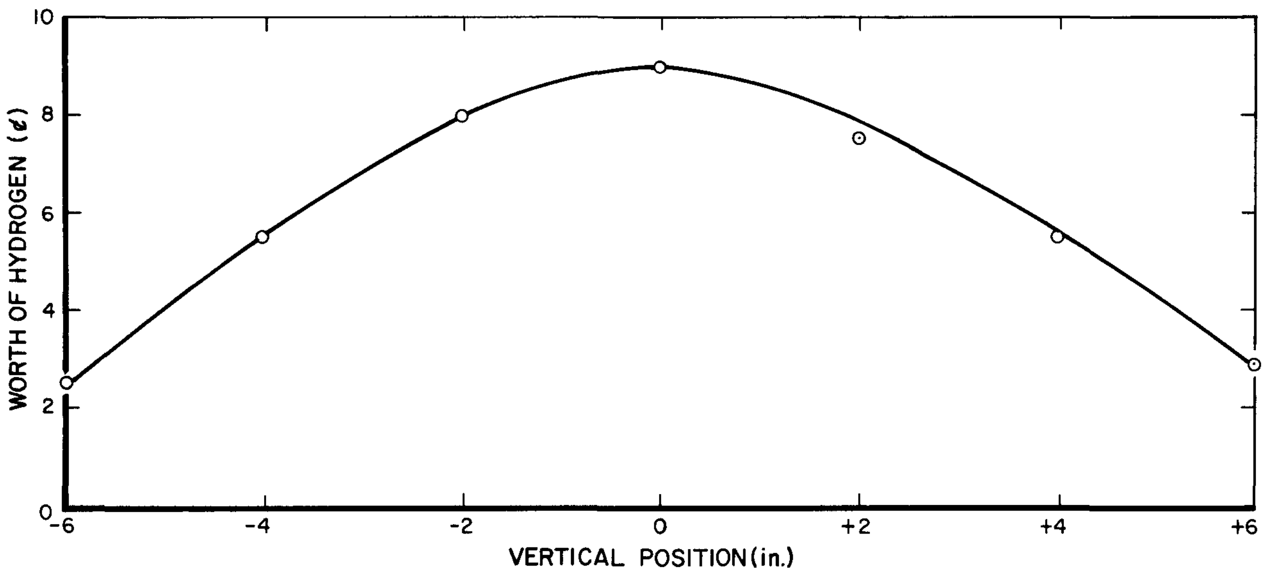

8-11-64 7568-01483

Figure 20. Axial Hydrogen Worth

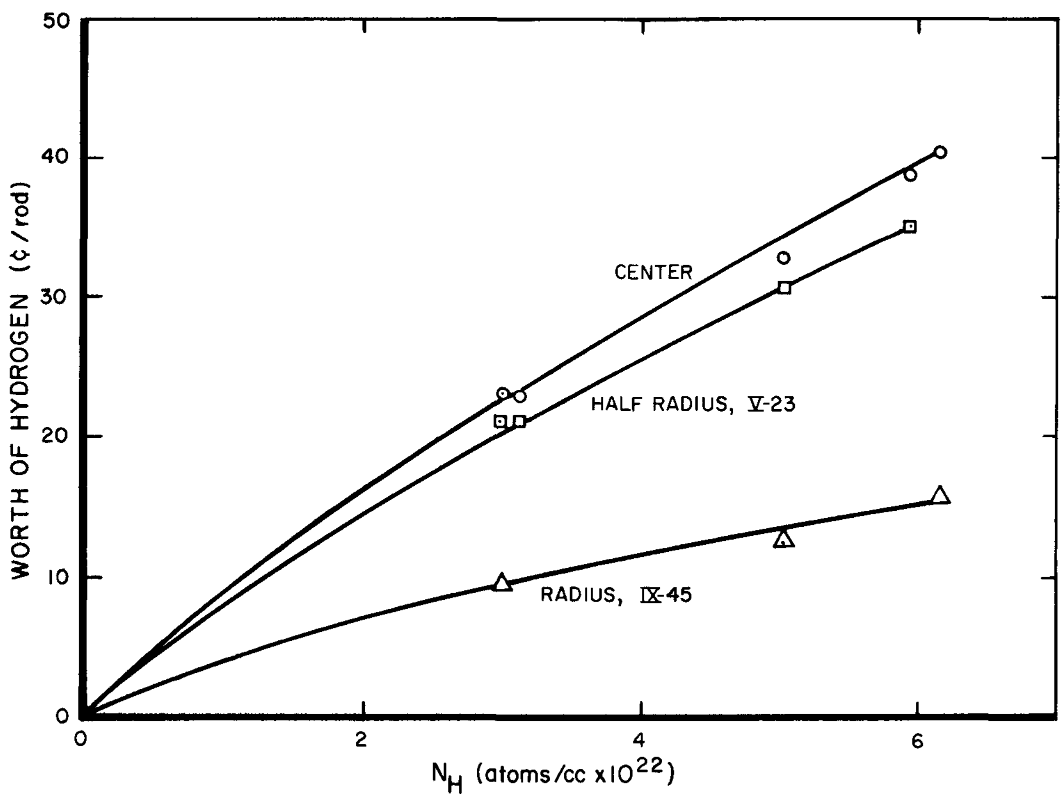

8-11-64 7568-01484

Figure 21. Radial Hydrogen Worth

uranium and hydrogen content. The top segment had an N_H of zero. U^{235} foils were placed between the segments, activated at low reactor power for 30 minutes, and subsequently counted with a scintillation counter. Standard corrections for background, decay, and foil weight were applied. For the radial measurement, the U^{235} foils were taped to the center of the sides of the fuel elements between the core center and Drum No. 3, which was fully inserted.

E. REACTIVITY WORTHS OF SPECIAL FUEL RODS AND ABSORBERS

To provide basic data for future analysis and interpretation of reactor performance at power and temperature, the worths of a range of fuel, moderator and poison densities in elements were measured. Special absorbers were evaluated for possible use in criticality control.

1. Variation in N_H and U^{235} Densities

The axial and radial variations in the reactivity worth of the hydrogen moderator were determined by measuring the differences between special fuel rods or rod segments having normal and zero hydrogen content.

Axial measurements were obtained at the core center (position I-1) using the segmented fuel rod described in Section III-D above. The worth of the zero N_H segment at the seven possible elevations is shown in Figure 20. The "normal" fuel segments had an N_H of 6.3×10^{22} atoms/cm^3.

Radial variations were determined by comparing complete fuel elements having nominal zero, 3.0, 5.0, and 6.0×10^{22} N_H densities at the core center (position I-1), at one-half the core radius (position V-23), and at the core periphery (position IX-45). The differences between the $N_H = 0$ element and the other elements give the worth of hydrogen in the respective rods. These differences are plotted in Figure 21.

For the central core position, the worths of different values of hydrogen concentration were predicted using the FAIM code to determine the calculated values. These values are compared to the experimental measurements in Table 5.

Standard fuel-moderator rods representing the range of normal manufacturing tolerances were placed in the core center position and their worths relative to a lucite rod and a void were measured. Zero N_H rods were measured relative to a void at the center, at one-half the core radius, and at the core periphery. Table 6 gives the results of the measurements and the composition of each rod.

TABLE 5

ROD WORTH WITH VARYING N_H AT CORE CENTER

N_H	Worth (¢)	
	Experiment	Calculated
0	0	0
3	22.6	20.8
5	34.1	35.1
6	39.6	41.6

TABLE 6

ROD WORTH WITH VARYING U^{235} AND N_H DENSITIES

Rod No.	Fuel Weight (gm)	N_H ($\times 10^{22}$)	Percent Uranium	Position	Worths (¢)	
					Relative to Lucite	Relative to Void
Lucite	70.64	-	-	I-1	-	45
E-181	309.3	5.97	9.70	I-1	1.4	46.4
E-672	311.5	6.27	9.95	I-1	4.3	49.3
E-669	317.3	5.97	10.11	I-1	5.8	50.8
E-671	293.9	6.15	9.32	I-1	3.5	48.5
E-661	278.0	0	9.54	I-1	-	11.5
E-660	278.3	0	9.78	V-23	-	9.0
E-661	278.0	0	9.54	V-23	-	10.0
E-661	278.0	0	9.54	IX-45	-	14.5

From the data in Figure 21 and Table 6, the approximate worth of a normal fuel rod relative to a void can be established for the three radial positions measured. The results are tabulated in Table 7 and compared to

TABLE 7

RADIAL VARIATION IN ROD WORTH

	Center	1/2 Radius	Periphery
Core position	I-1	V-23	IX-45
Hydrogen worth, ¢	39.6	35.0	15.0
Uranium worth, ¢	11.5	10.0	14.5
Fuel rod worth, ¢	51.1 ± 3	45.0 ± 3	29.5 ± 3
Calculated worth, ¢	60	52.5	27.5

the rod worths calculated by the FAIM code. The uncertainty of ±3¢ in the measured values represents the estimated range manufacturing and experimental tolerances.

2. Burnable Poison Coating

The poison worth of the ceramic Sm_2O_3 coating inside the fuel element cans was determined for one and for two empty cans at the core center. An empty, uncoated fuel can was worth -1¢, and the coatings were worth -2.5¢ and -4.3¢ for one and two cans respectively. A straightforward averaging of the measured coating worths yields -2.3¢/can at the core center.

3. Samarium Worth

A simple experiment was devised to obtain a rough measurement of the reactivity coefficient of samarium oxide, i.e., worth/gram Sm_2O_3. A 0.107-gm sample of Sm_2O_3 was sandwiched in a thin layer between aluminum foil and Scotch tape to minimize self-shielding effects. This ribbon-like sample was supported in an uncoated fuel can and the worth was measured at two core locations as shown in Table 8.

TABLE 8

WORTH OF SAMARIUM OXIDE

Core Position	0.107 gm Worth	Worth/gm Sm_2O_3
I-1	-3.5¢	-33¢
V-23	-3.4¢	-32¢

Assuming the worth at the half-radius position V-23 is representative of the core average worth, the initial worth of the Sm_2O_3 burnable prepoison is calculated as follows:

$$-32 \frac{\text{cents}}{\text{gm } Sm_2O_3} \times 8.51 \text{ gm } Sm_2O_3 = -272 \text{ cents}$$

Prepoison worth was predicted originally to be -338 cents based on an initial core loading of 10.11 gm Sm_2O_3. By further assuming a linear relationship between core loading and poison worth, the as-built predicted Sm_2O_3 worth is -285 cents. The agreement between the two values is remarkable and may be fortuitous considering the simplifying assumptions. However, extension of this analysis to the coating measurements of Section III-E-2 above produces a similar agreement. The as-built predicted worth of the central can coating is -2.2 cents compared to the -2.3 cents measured.

4. Boron Worth

The reactivity coefficient measurement described above for Sm_2O_3 was repeated to determine boron worth and, in addition, the worth of a boron-filled rod at the core center was measured. The test conditions and results are shown in Table 9 below.

TABLE 9

BORON WORTH AT CORE CENTER

	Ribbon	Rod
Weight boron, gm	0.1966	16.04
Measured worth, ¢		
Relative to void	-9.5	-182
Relative to fuel	---	-232
Worth 1 gm boron, ¢	-48	-11

The self-shielding effects of the rod are evident.

5. Worth of Poison Splines

The worths of special poison splines, proposed for criticality control during subsequent experiments, were determined in several different arrays. The splines were 1/16-in.-OD tubing filled with 1 to 2 gm of a mixture of rare earth oxides. A single spline could be inserted in the void region between any three adjacent fuel elements and would provide control over the entire length of the fuel elements. The results are tabulated in Table 10. Comparative worths calculated using the ULCER code are included and are in good agreement with the values measured. The interaction or shadowing effects of adjacent splines appear to be negligible.

TABLE 10

WORTH OF POISON SPLINES

Spline Array	Total Weight of Poison (gm)	Worth (¢)		Average Spline Worth (¢)
		Measured	Calculated	
1 centered	2.05	-8	---	-8
6 clustered around center rod	12.1	-52.5	-51.1	-8.8
6 clustered around rod VI-26	12.1	-36.0	---	-6.0
6 distributed between fuel rings VI and VII	12.1	-34.5	-40.2	-5.8
19 uniformly distributed over the core	34.56	-146.5	-130.5	-7.7

F. REACTIVITY WORTH OF INTERNAL REFLECTOR INSERTS

Three of the BeO internal reflector inserts along the flat of the core adjacent to Drum No. 4 were individually and collectively removed to determine their worth relative to a void. The resultant measurements and the worths calculated by ULCER are shown in Table 11.

The relatively large discrepancy between measurement and calculation is attributed to the differences between the experiment and the analytical model. The core-reflector interface region of the model is symmetrical in the angular direction. Thus, the effect of removing one or more inserts is uniformly

TABLE 11

WORTH OF BeO INTERNAL REFLECTORS

Insert Removed	Worth (¢)	
	Measured	Calculated
First flat insert	-12	-19.5
Second flat insert	-15	-21.1
D insert	-6.3	-8.7
All three inserts	-34.7	-47.7

smeared over the entire interface region. The analytical model does reveal a distinct non-linearity in the worths of successive removals of reflector inserts. The experimental worth of all 18 inserts is $4.50, extrapolated by means of the ULCER code from the measurement of 3 inserts.

G. PILE NOISE MEASUREMENTS

Using the methods described in Reference 5, the measured β_{eff}/ℓ^* ratio was 950 sec^{-1} ±10% compared to a calculated value of 1060 sec^{-1}. The value deduced for the mean prompt neutron lifetime, ℓ^* is 8.1×10^{-6} sec, assuming the calculated effective delayed neutron fraction of 0.0077.

H. TOTAL EXCESS REACTIVITY

The excess reactivity of the S8ER may be inferred directly for two shim configurations from measurements obtained with the fully fueled core. The first of these is loading C-3 described in Table 2, and the second measurement was a critical drum configuration with the A-B shims installed.

Loading C-3 was a subcritical configuration with no reflector shims installed. The critical loading extrapolated to 213.2 fuel elements, 2.2 elements more than the fully fueled reactor. Both calculations and measurements indicate that the average worth of peripheral fuel relative to lucite is approximately 13¢ per element. Therefore Loading C-3 has an excess reactivity of -(2.2 x 13¢) = -28¢.

The critical configuration determined with the A-B shim was obtained with Drum No. 1 locked OUT, Drum No. 5 at 41.4°, and the remaining drums IN.

Assuming that the Drum No. 1 and Drum No. 5 calibrations are identical because of the adjacent-drums-IN symmetry considerations, the excess reactivity is deduced as follows:

Drum No. 1 OUT	\$3.67
Drum No. 5 @ 41.4°	2.33
A-B Shim Excess Reactivity	\$6.00

Using these two measured excess reactivity values and the six-shim worths of Table 3, the S8ER cold, dry excess reactivity as a function of effective reflector thickness is determined as shown in Table 12. The measured and calculated values of K_{eff} are included. ULCER was used to determine the calculated values which are in reasonable agreement with the measurements. For completeness, rough approximations of the total drum worth and subcritical margins are listed. These total drum worths are simply the measured single drum worths multiplied by six with no allowance made for drum interaction.

TABLE 12

S8ER EXCESS REACTIVITY

	Effective Reflector Thickness (in.)				
	2.34	3.08	3.78	4.73	4.47
Shim configuration	None	A	A-B	A-C-B	A-B-B
Excess reactivity, \$	-0.28	3.24	6.00	8.46	7.71
Excess reactivity, %Δk/k	-0.22	2.49	4.62	6.51	5.94
Measured K_{eff}	0.9978	1.026	1.048	1.070	1.063
Calculated K_{eff}	1.001	1.033	1.056	1.079	1.074
Approximate total drum worth, \$	-	20.20	22.00	21.35	-
Approximate subcritical margin, \$	-	17.00	16.00	12.90	-

BLANK

IV. CONCLUSIONS

The nuclear characteristics of the dry S8ER core were determined to confirm and refine the calculational techniques used in the design of SNAP reactors and to provide data to define and interpret subsequent reactor experiments.

The best calculated values of reflector worth appear to be those obtained using ULCER rather than FAIM. However, the FAIM code provides reliable values for the reactivity effects of fuel rods and absorbers within the core.

As a result of these experiments, a modified A-C-B shim configuration was installed in the power test facility to provide sufficient excess reactivity plus some contingency for S8ER operations at power.

Future beryllium-reflected reactor experiments should provide for direct determination of the weights and impurities of the Be and BeO components. This information will aid in resolving and understanding the experimental-calculational differences encountered here.

BLANK

[redacted]

REFERENCES

1. D. S. Brinkman and V. L. Rooney, NAA-SR-7261, "Snap 8 Experimental Reactor, A Description," (Confidential), (June 15, 1962)

2. R. S. Randall and C. W. Griffin, "Application of Power Spectra to Reactor System Analysis," *Transactions of the Symposium on Noise Analysis in Nuclear Systems* (Univ. of Florida, 1963)

3. H. J. Hubbell and W. E. Nagel, NAA-SR-8589, "Snap 8 Experimental Reactor Fuel Element Acceptance Testing," (Secret), (March 1, 1964)

4. D. C. Baller, NAA-SR-7137, "The FAIM Code, a Multigroup, One-dimensional, Diffusion Equation Code," (Unclassified), (January 1962)

5. D. S. Vargofcak, W. T. Hayes, and D. W. Roeder, "ULCER, a One-Dimensional Multigroup Diffusion Equation Code with Upscatter," NAA-SR-MEMO-9891 (Unclassified), (May 1964)

SECRET